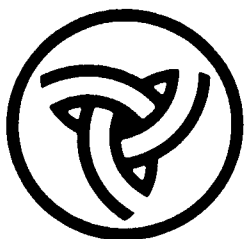
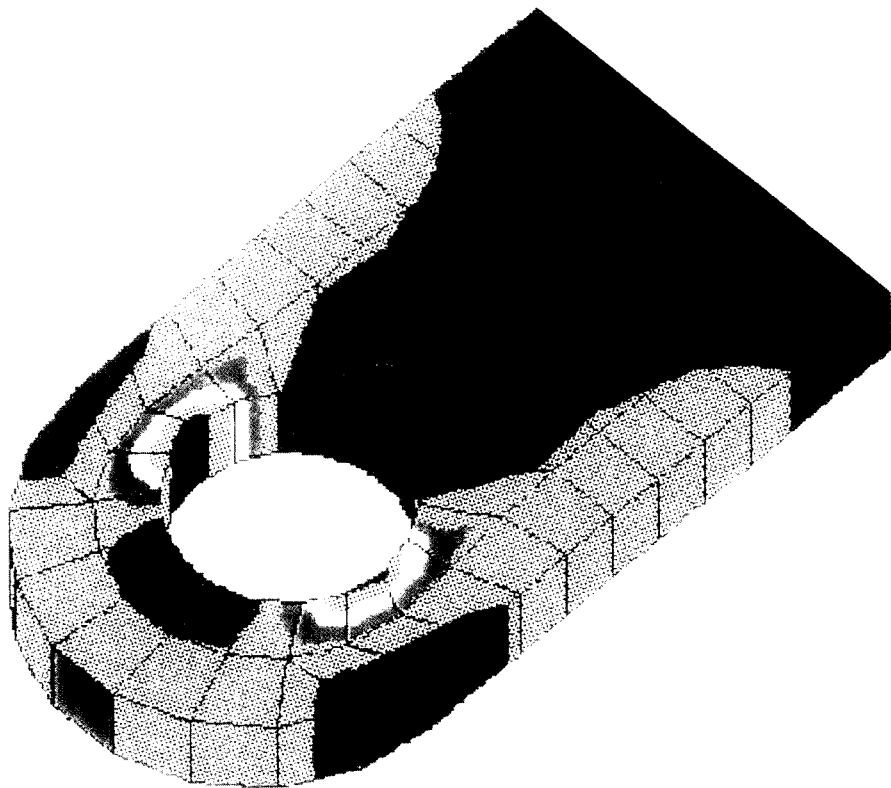


Analysis, Inspection, And Repair Methods For Pin Connections On Illinois Bridges

Physical Research Report No. 107



Illinois Department of Transportation

Bureau of Materials and Physical Research

1. Report No. FHWA/IL/PR-107	2. Government Accession No.	3. Recipient's Catalog No.	
4. Title and Subtitle Analysis, Inspection, and Repair Methods for Pin Connections on Illinois Bridges.		5. Report Date April, 1992	
		6. Performing Organization Code	
7. Author(s) J. M. South, C. Hahin, R. O. Telford		8. Performing Organization Report No. PRR-107	
9. Performing Organization Name and Address Illinois Department of Transportation Bureau of Materials and Physical Research 126 E. Ash Street Springfield, IL 62704-4766		10. Work Unit No. (TRAIS)	
		11. Contract or Grant No.	
12. Sponsoring Agency Name and Address Illinois Department of Transportation Bureau of Materials and Physical Research 126 E. Ash Street Springfield, IL 62704-4766		13. Type of Report and Period Covered Final Report 6/88 to 6/91	
		14. Sponsoring Agency Code	
15. Supplementary Notes Study conducted in cooperation with the U. S. Department of Transportation, Federal Highway Administration.			
16. Abstract <p>This report documents methods used in Illinois for analysis, inspection, and repair of pin connections in bridges. Weldable foil strain gages were used to detect the effects of unknown levels of fixity in pins on cantilever truss bridges. Other methods for detecting pin movement, including electronic angle sensors and scratch-type pointer gages were also investigated. The maximum effect of complete fixity on pins and hangers was estimated with finite element models of both cantilever truss and cantilever girder bridges. A pin inspection procedure using ultrasonic instrumentation was developed and tested throughout the state. Design deficiencies of pin connections are noted. Modernized details which eliminate many of the existing deficiencies are presented. The improvements include better tolerances on fits and finishes, increased degrees of freedom of rotation, provisions for periodic lubrication, high strength, corrosion resistant alloys, extreme pressure lubricants, and toughness requirements based on alloy yield strength. A method for calculating factor of safety for pins based on distortion energy principles is presented.</p>			
17. Key Words Pin connections, strain gages, finite element models, pin inspection, ultrasonic testing, safety factors, modernized pin details.		18. Distribution Statement No restrictions. This document is available to the public through the National Technical Information Service, Springfield, VA 22161	
19. Security Classif. (of this report) Unclassified	20. Security Classif. (of this page) Unclassified	21. No. of Pages 100	22. Price

ANALYSIS, INSPECTION, AND REPAIR METHODS
FOR
PIN CONNECTIONS ON
ILLINOIS BRIDGES

by

Jeffrey M. South, P. E.
Structural Analyst
Bureau of Materials and Physical Research

Christopher Hahin, P. E.
Engineer of Bridge Investigations
Bureau of Materials and Physical Research

Richard O. Telford, P. E.
Bridge Inspection Engineer
Bureau of Maintenance

ILLINOIS DEPARTMENT OF TRANSPORTATION
BUREAU OF MATERIALS AND PHYSICAL RESEARCH
APRIL 1992

The contents of this report reflect the views of the authors who are responsible for the facts and the accuracy of the data presented herein. The contents do not necessarily reflect the official views or policy of the Federal Highway Administration or the Illinois Department of Transportation. This report does not constitute a standard, specification, or regulation.

NOTICE

Neither the United States Government nor the State of Illinois endorses products or manufacturers. Trade or manufacturers' names appear herein solely because they are considered essential to the object of this report.

TABLE OF CONTENTS

	<u>PAGE</u>
List of Figures	i
List of Tables	v
1 Introduction	1
2 Detecting Pin Movement	4
3 Finite Element Analysis	15
4 Experimental Stress Analysis	26
5 Ultrasonic Pin Inspection	31
6 Existing Pin & Link Design; Retrofit Replacement	51
7 Summary	78
8 Conclusions	81
References	83
Appendices	

LIST OF FIGURES

<u>FIGURE NO.</u>	<u>DESCRIPTION</u>	<u>PAGE</u>
1	Photograph of paper gage installed on hanger on I-270 over Chain-of-Rocks Canal near Granite City, Illinois.	5
2	Photograph of a mechanical, scratch-type pointer installed on I-55 over Illinois Route 29 at Springfield, Illinois.	7
3	Photograph of a scratch-type pointer gage and a pointer with a calibrated scale installed on I-474 over the Illinois River at Peoria.	8
4	Strain gage installation for detection of bending strains induced by pin fixity.	9
5	Photograph of weldable strain gages installed on a hanger on I-270 bridge.	10
6	Photograph of an electronic angle sensor installed on Hazel Dell Road over I-55 in Springfield.	12
7	I-270 over Chain-of-Rocks Canal. Bridge is symmetrical about the centerline.	17
8	Finite element approximation of a truss section near a hanger on I-270 over Chain-of-Rocks Canal. Pins are located at nodes M13 and G13.	18
9	Static deflection diagram of lower chord of I-270 bridge, without deadload effect.	19
10	Hazel Dell Road over I-55 in Springfield, Illinois.	24
11	Wheatstone bridge circuit diagram for measurement of bending strains with insensitivity to axial strains.	27
12	Distance and Sensitivity Calibration-Pin (DSC-P) calibration block developed for use with pin inspections.	33
13	Photograph of pin with deep wear grooves.	36

LIST OF FIGURES, CONT'D

<u>FIGURE NO.</u>	<u>DESCRIPTION</u>	<u>PAGE</u>
14	Ultrasonic test data for an actual 3-inch diameter pin specimen using a straight beam transducer. Figure shows unadjusted data, results from IDOT procedure, and results from IDOT procedure without distance attenuation correction factor.	43
15	Ultrasonic test data for an actual 3-inch diameter pin specimen using a 20 degree angle beam transducer. Figure shows unadjusted data, results from IDOT procedure, and results from IDOT procedure without distance attenuation correction factor.	44
16	Ultrasonic test data for an actual 3-inch diameter pin specimen using a 30 degree angle beam transducer. Figure shows unadjusted data, results from IDOT procedure, and results from IDOT procedure without distance attenuation correction factor.	45
17	Ultrasonic test data for an actual 3-inch diameter pin specimen using a 45 degree angle beam transducer. Figure shows unadjusted data, results from IDOT procedure, and results from IDOT procedure without distance attenuation correction factor.	46
18	Ultrasonic test data for a plate specimen of ASTM A572 steel using a straight beam transducer. Pertinent specimen geometry was the same as that of the tested pin specimen. Figure shows unadjusted data, results from IDOT procedure, and results from IDOT procedure without distance attenuation correction factor.	47
19	Ultrasonic test data for a plate specimen of ASTM A572 steel using a 20 degree angle beam transducer. Pertinent specimen geometry was the same as that of the tested pin specimen. Figure shows unadjusted data, results from IDOT procedure, and results from IDOT procedure without distance attenuation correction factor.	48

LIST OF FIGURES, CONT'D

<u>FIGURE NO.</u>	<u>DESCRIPTION</u>	<u>PAGE</u>
20	Ultrasonic test data for a plate specimen of ASTM A572 steel using a 30 degree angle beam transducer. Pertinent specimen geometry was the same as that of the tested pin specimen. Figure shows unadjusted data, results from IDOT procedure, and results from IDOT procedure without distance attenuation correction factor.	49
21	Ultrasonic test data for a plate specimen of ASTM A572 steel using a 45 degree angle beam transducer. Pertinent specimen geometry was the same as that of the tested pin specimen. Figure shows unadjusted data, results from IDOT procedure, and results from IDOT procedure without distance attenuation correction factor.	50
22	Typical new 9-inch diameter pin connection detail.	57
23	Special wrench for torque application. Overtightening causes the loading pin to shear off.	59
24	Nut and seal detail for moisture exclusion.	60
25	Nine-inch diameter pin detail also showing material properties and surface finish requirements.	61
26a	Detail drawing of link plate.	62
26b	Finite element model of the link eyebar. Stresses are for maximum loadings for the Peru Bridge. Note that eyelet stresses are about 3X nominal stress. Stress values in the legend are in psi.	64
27	Machined and finely ground pins for Peru Bridge.	69
28	Closeup of pin and general size.	69
29	Circular nuts for pins. All grooves and holes for dog bolts were not yet machined out.	70

LIST OF FIGURES, CONT'D

<u>FIGURE NO.</u>	<u>DESCRIPTION</u>	<u>PAGE</u>
30	Special chamfer which permits a space for a grease seal situated between the nut and link eyebar.	70
31	Machined link eyebars, milled to be completely flat and with radii with smooth finishes. Bearings have not yet been inserted in this picture.	71
32	A stack of four bronze inserts, showing internal grease groove.	72
33	Principal forces and stresses on pins and link eyebars.	74
34	Stress factor for typical eyebar design (Ref. 4, page 376).	75

LIST OF TABLES

<u>TABLE NO.</u>	<u>DESCRIPTION</u>	<u>PAGE</u>
1	Torque and torsional shear stress on seven-inch diameter pins (I-270) completely fixed.	20
2	Torque and torsional shear stress on twelve-inch diameter pins (I-474) completely fixed.	22
3	Strain gage data and analysis for I-270 bridge.	29
4	Strain gage data and analysis for I-474 bridge.	29
5	Distribution of structures with fracture critical appraisal ratings of 0-8.	37
6	Ultrasonic data for notches of known depth and location in an actual pin.	40
7	Ultrasonic data for notches of known depth and location in plate specimens.	41
8	Various standard pin geometries now in use.	53
9	Pin, link, and bearing alloys.	65
10	Pin and link lubricants.	66
11	Impact toughness requirements for pin and link materials for Temperature Zone 2.	68
12	Typical coefficients of static friction.	76

1. INTRODUCTION

The nearly catastrophic failure of several pins in a bridge on I-55 in St. Louis, Missouri in 1987 and other incidences of pin failures throughout the country such as the collapse of the Mianus River Bridge on I-95 in Connecticut prompted the Federal Highway Administration (FHWA) to require inspection of all pins and pinned connections in bridges throughout the country. This report documents efforts by the Illinois Department of Transportation to define the problem in Illinois, quantify the forces and moments involved, develop methods to detect pin movement, inspect pins for defects, and develop improved pin connection details. This work was accomplished through a joint effort by personnel from the Bureaus of Bridges and Structures, Maintenance, Materials and Physical Research, Local Roads and Streets, and the FHWA in the form of a Technical Advisory Committee (TAC).

In general, there are three types of pinned connections used in Illinois. Large pins (typically seven inches in diameter and greater) are used in hangers on cantilever truss bridges. An example of this type of bridge is I-270 over the Chain-of-Rocks Canal near Granite City, Illinois. Smaller pins (less than five inches in diameter) are used in conjunction with link eyebars to support the end spans of many cantilever girder bridges throughout the state. Small pins without hanger straps are also used as a moment-relief mechanism in some bridges. In this report, hangers refer to members in cantilever truss bridges and links or link eyebars refer to components in cantilever girder bridges.

Pins and hangers or link eyebars are normally designed to resist shear and bending stresses induced by dead load and traffic. The connection is assumed upon installation to be torsion-free. This assumption may be valid when the bridge is new, but after years of exposure to atmosphere, deicing salts, and load variations, corrosion and wear tend to produce at least a partially fixed condition in the pin connection. This fixity induces shear stresses in both the pin and link eyebar during expansion and contraction of the bridge with temperature and can also produce shear stresses due to live load, especially in cantilever girder bridges. The combination of inadequate design for torsion accompanied by corrosion and wear of a pin produces undesirable stress states that can cause internal and external defects, flaws and discontinuities to develop and grow either in the pin or the hanger/link eyebar. The initiation and growth of a crack in a fracture critical detail such as a pin or a link eyebar can lead to catastrophic failure.

The number of pins in Illinois bridges that are susceptible to damage is large. According to data compiled by the TAC, there are approximately 130 cantilever girder bridges with pin-link eyebar, or pin-plate details (small pins) in Illinois. There are a total of 3,165 pins in these bridges. There are fifteen cantilever truss bridges in Illinois with 120 large pins.

As indicated by Carroll, et al.,¹ of the Missouri Highway and Transportation Department, visual inspection of pins for defects is inadequate, because the areas of corrosion and wear are inaccessible while under load. Prior to this research, Illinois had no experiment-based procedures to either determine fixity or adequately inspect pins for defects. In order to comply with the FHWA directive, methods for determining fixity and for pin inspection were developed.

Retrofit details were developed which allow free movement, moisture exclusion, and galling and corrosion resistance.

2. DETECTING PIN MOVEMENT

In order to better analyze pin behavior in a partially fixed or fixed configuration, it was essential to detect pin movement to help quantify the forces, moments, and stresses involved. Several methods of detecting pin and/or hanger movement were developed which ranged from simple to sophisticated. These methods included 1) paper gages, 2) paint stripes, 3) pointers, 4) strain gages, and 5) electronic rotation sensors.

Paper Gages

The paper gage consisted of a 2 x 6-inch strip of paper with a 1/8 inch wide black strip running down the longitudinal centerline. It was installed by gluing both ends to a hanger-gusset interface and then cutting the paper between. The theory was that relative motion (temperature-induced) would be visible by relative displacement of the black strip. A picture of an installation on the I-270 Bridge is shown in Figure 1. Several drawbacks were noted for this idea: 1) installation was difficult, 2) even when waterproofed, the paper tended to curl and degrade over a short time, 3) the gages were often covered with bird droppings and damaged by maintenance activities, especially by bridge cleaning with water spray, 4) the method was not very sensitive, and 5) a quantitative analysis of pin fixity was not possible.

Paint Stripes

Paint stripes were conceived as a refinement to paper gages. A piece of masking tape was put in place of the paper gage and sprayed with a fast-drying black paint. The tape was then removed. This solved the



Figure 1. Photograph of paper gage installed on hanger on I-270 over Chain-of-Rocks Canal near Granite City, Illinois.

installation problem, but did not alleviate the others. Detecting motion was difficult.

Pointers

Several types of mechanical pointers were investigated. These pointers recorded movement by scratching the paint on the bridge. Several of these pointers were installed on I-55 over Illinois Route 29 at Springfield. See Figure 2. Installation was not difficult, although holes had to be tapped into either the pin or the nut which could interfere with an ultrasonic inspection. Detection of small movement was difficult.

Another type of pointer, which included a calibrated angle scale, was installed on a bridge near Peoria. See Figure 3. This pointer also required holes to be tapped. Installation was more complicated, since the graduated scale had to be positioned carefully. Detection of small movement was still difficult.

Strain Gages

An electrical resistance strain gage installation was designed to measure bending stresses in a hanger or link eyebar while being insensitive to axial stresses.² See Figure 4. The theory behind this method was that free pins would not introduce any bending stresses into the hanger, while partially fixed and fixed pins would induce some degree of bending. Several hangers on the I-270 bridge and I-474 over the Illinois River at Peoria were instrumented in this fashion. See Figure 5. This method has the advantage of being extremely sensitive to bending stresses. The major drawbacks of this idea were: 1) strain gages can be

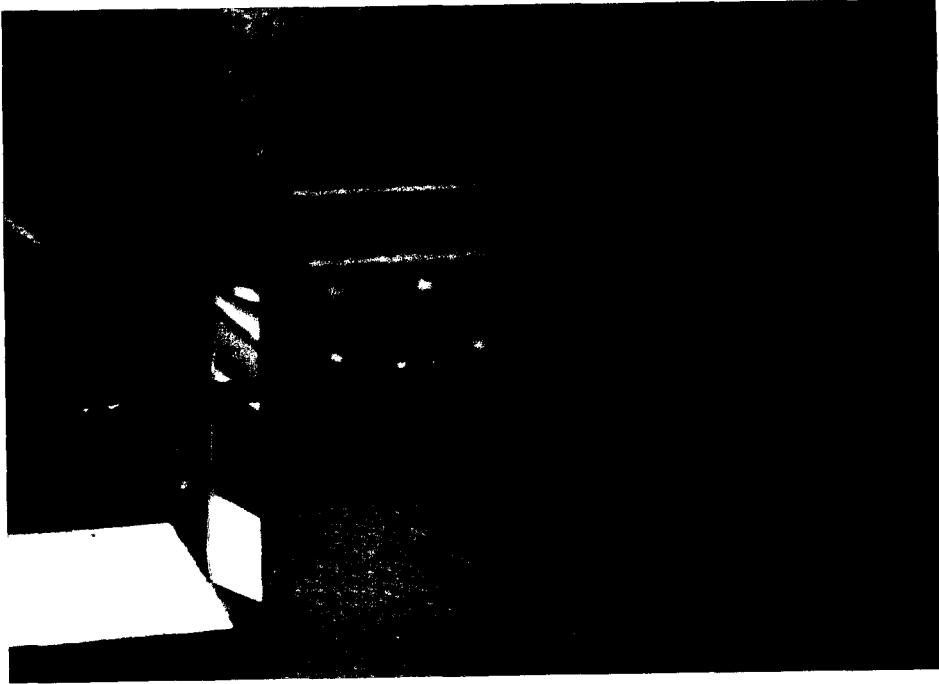


Figure 2. Photograph of a mechanical, scratch-type pointer installed on I-55 over Illinois Route 29 at Springfield.

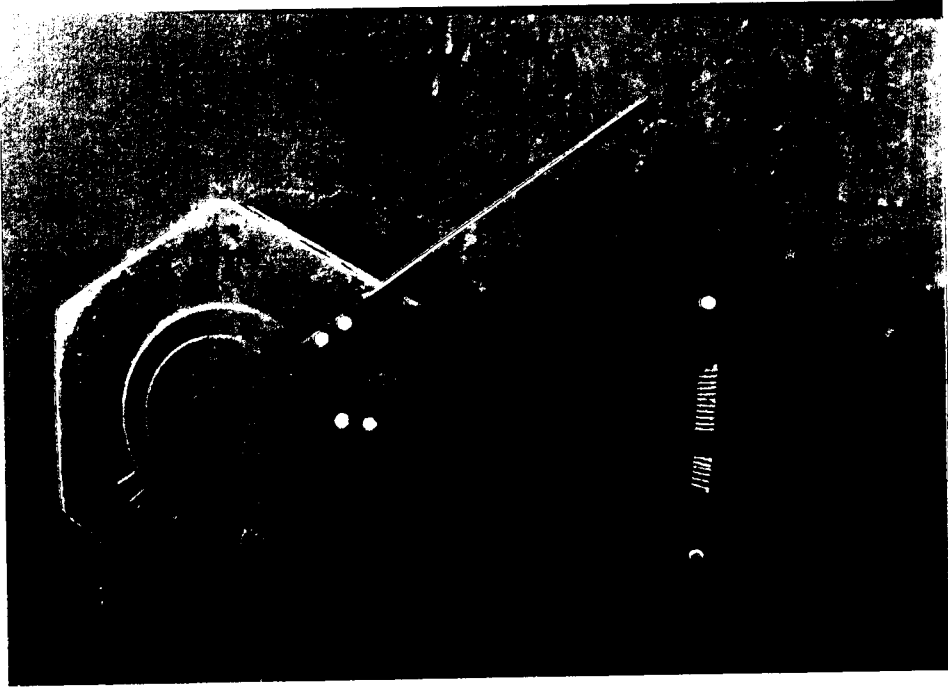
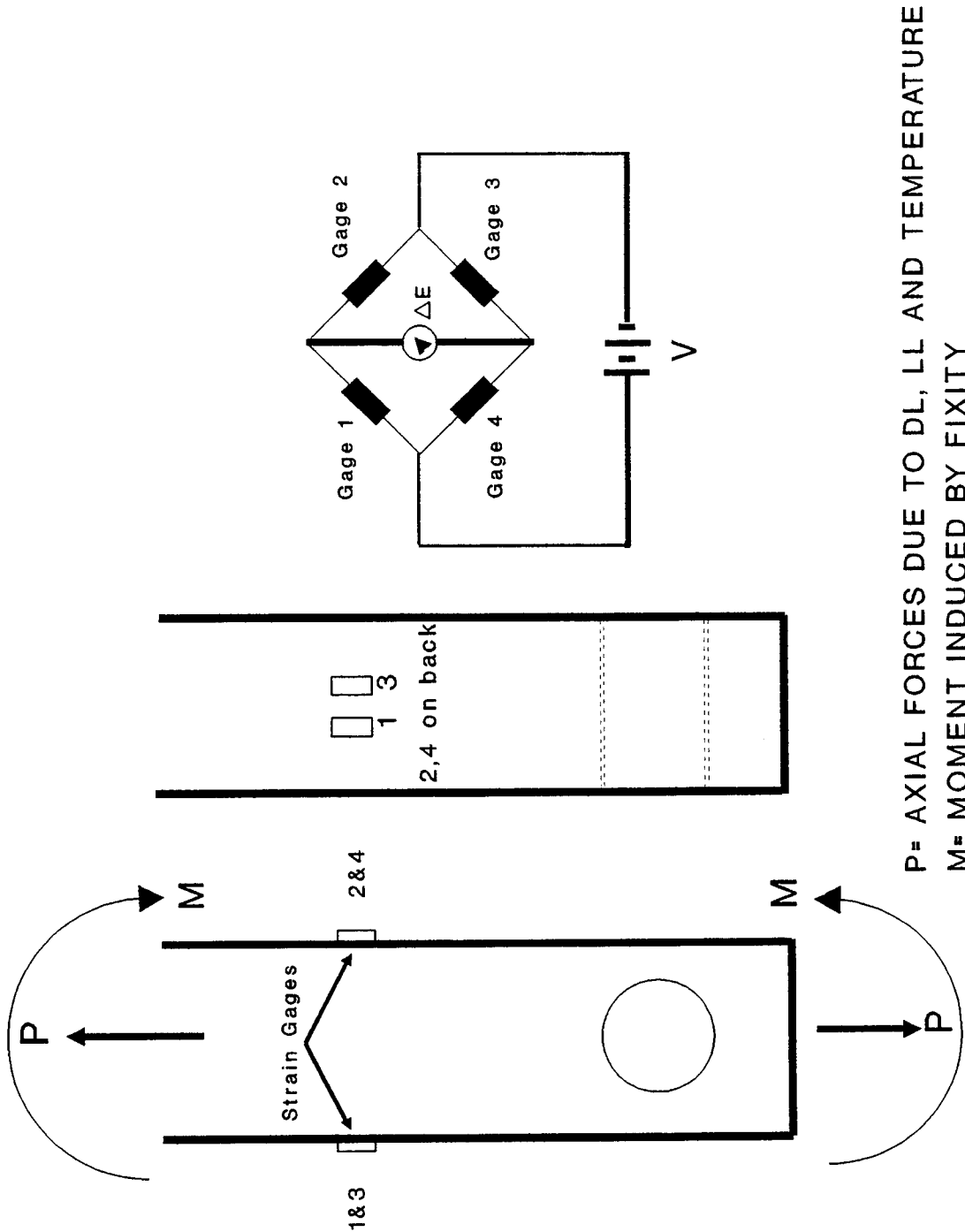


Figure 3. Photograph of a scratch-type pointer gage and a pointer with a calibrated scale installed on I-474 over the Illinois River at Peoria.



P= AXIAL FORCES DUE TO DL, LL AND TEMPERATURE
M= MOMENT INDUCED BY FIXITY

Figure 4. Strain gage installation for detection of bending strains induced by pin fixity.



Figure 5. Photograph of weldable strain gages installed on a hanger on I-270 bridge.

difficult for untrained individuals to properly install and wire, 2) special equipment is necessary to take accurate readings, and 3) this method would be more difficult to apply to small links.

Electronic Rotation Sensors

An electronic angle sensor was used in conjunction with the pointer gage to provide sensitivity, accuracy and repeatability. The angle sensor was mounted on the pointer arm. Rotation was detected by recording an initial reading at a given temperature, then returning for another reading when a large temperature change occurred. The problem of tapping holes in a pin reduces the viability of this method. This method was able to detect very small relative rotations of the order of 0.1 degrees. Another type of angle sensor was fitted with magnets so that it could be mounted directly to the link eyebar. See Figure 6. This configuration does not require any holes, but the instrument must be left in place for the complete test. Two drawbacks of rotation sensors are their cost and the fact that further stress analysis on pins and hangers or link eyebars is difficult.

Loaded Truck Quick-Stop Test

The biggest problem with all of the methods described is that the movement to be measured is induced by temperature change; hence the best comparisons are made between summer and winter. This "time delay" aspect of the previous methods renders them all undesirable from the point of view of obtaining a fast, accurate answer on fixity. The use of angle sensors in conjunction with a loaded truck to induce pin and/or link eyebar movement in cantilever girder bridges was investigated as a

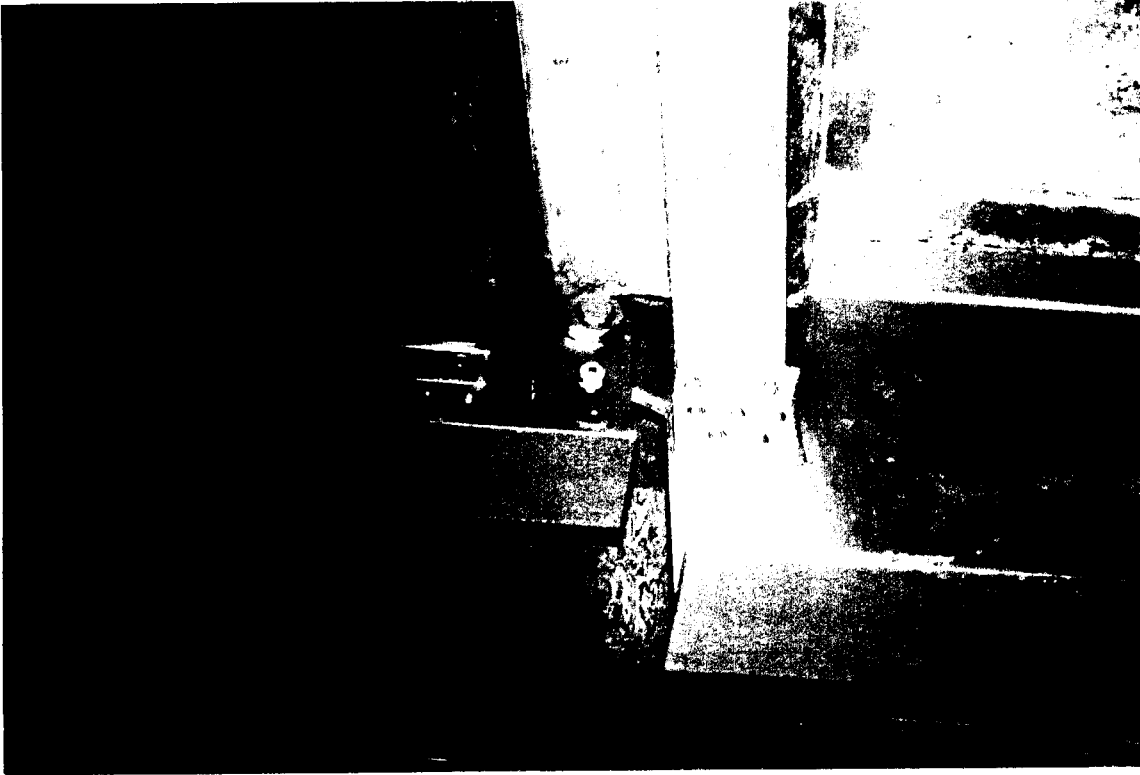


Figure 6. Photograph of an electronic angle sensor installed on Hazel Dell Road over I-55 in Springfield.

"quick-stop test" method. The equipment consisted of an angle sensor, a chart recorder and a calibration box. The theory was that a loaded truck (15-20 tons) could be driven onto the suspended span of the bridge and stopped quickly to induce a longitudinal force into the bridge. The angle sensors would measure any relative rotation between pin, link eyebar, and stringer and these changes could be quantified by recording them on a chart recorder and referencing to a calibration input. The applicability of this method is restricted to bridges with relatively few pin connections, since the larger the bridge, the less force transmitted to each individual pin. Preliminary results using this method were not promising and the method was abandoned.

Results

After a very short exposure, the paper gages and paint stripes were either completely degraded by weather or covered with bird droppings. These methods produced no meaningful results and are not recommended for use. The pointers worked slightly better, but still did not produce meaningful data. The major drawbacks of the pointer method are that holes must be drilled and tapped in either the pin or nut in order to anchor the pointer and that further stress analysis is not possible. A hole in the end of a pin severely interferes with ultrasonic inspection. This method, therefore, is not recommended for use. The strain gages installed on large hangers worked well, with the exception of some problems with weatherproofing, which are easily corrected. A strain gage circuit was also designed for link eyebars but was not field tested. Meaningful data were produced by the strain gage method, as shown in Chapter 4. This method is recommended for use as an analysis tool for

tracking fixity in cantilever truss bridges. The method would be useful on cantilever girder bridges as well, given proper access for gage installation.

The electronic rotation sensors were also able to provide meaningful information, although less so than the strain gages. The question of rotation is answered, but further stress analysis is more difficult. Electronic rotation sensors are also much more expensive than strain gages. The "quick-stop test" method did not work, probably because the vehicle was too light and could not induce movement. Electronic rotation sensors are not recommended for general application but are useful for spot checks for thermal movement, especially at trouble spots on cantilever girder bridges.

Overall recommendations are the use of strain gage installations, especially on cantilever truss bridges, and spot use of electronic rotation sensors on cantilever girder bridges. The practicality of installing strain gage circuits on cantilever girder bridges remains to be seen due to structure redundancy and level of effort needed to instrument each bridge.

3. FINITE ELEMENT ANALYSIS

In order to generate approximate quantitative data on the maximum expected torques and stresses resulting from complete pin fixity, three finite element models were made using two cantilever truss bridges and one cantilever girder bridge. The cantilever truss bridges modeled were I-270 over the Chain-of-Rocks Canal and I-474 over the Illinois River at Peoria. The cantilever girder bridge modeled was Hazel Dell Road over I-55 in Springfield. The finite element program used was STRUDL.

Simulation of Pins in the Finite Element Analysis

A finite element model contains two types of nodes; free nodes and support nodes. Free nodes experience displacements and/or rotations according to structural analysis type. Free nodes in a truss analysis disregard rotations since the truss assumption allows only axial forces. Free nodes in a frame analysis may experience both displacements and rotations. Support nodes are the points in the model which support the model in space (e.g. piers and abutments). In a mathematical sense, support nodes are where displacement or rotation boundary conditions are applied. Support nodes may be modified to act as rollers, fixed points with rotation allowed, elastically supported points or completely clamped points. Support nodes experience reaction loads. Since the object of the finite element analysis was to estimate loads on pins, the bridge pins in the computer models were simulated by defining them as support nodes. All displacements were released in order to simulate a free node. The no fixity condition was simulated by allowing all rotations. The full fixity condition was simulated by restricting the rotations.

I-270 Over Chain-of-Rocks Canal

The truss section of the Chain-of-Rocks Canal bridge is 960 feet long. The cantilevered portion is 150 feet long, and the suspended span is 180 feet long. The structure was built circa 1960. The truss members are riveted box sections and were modeled using line elements. Since the truss members have oval holes (approximately 8 x 16 inches) cut in them on approximately three-foot spacings, the net section properties were used in the model for each individual member. Stringers, diaphragms, and floorbeam flanges and stiffeners were also modeled as line elements. The floorbeam webs and the concrete deck were modeled with hybrid elements which are a combination of plate bending and plane stress/plane strain elements. Only half of the structure was modeled in order to take advantage of symmetry. See Figure 7. Figure 8 shows a section of the bridge as a finite element approximation. Pins are located at nodes M13 and G13. The model was checked graphically to check the accuracy of the input geometry data and was subjected to various static loadings to check overall displacement behavior. See Figure 9. Movement due to temperature change was checked with simplified calculations (using a constant coefficient of thermal expansion). The computer output for thermal movement was within three percent of the simplified calculation. This check does not necessarily prove either method to be correct, but the close approximation of the two solutions indicates no gross modeling errors. The torque on the pins for a temperature change of 50°F was generated by the computer model and the resulting torsional shear stress on the seven-inch diameter pins (ASTM A237 Class A Steel) was calculated from

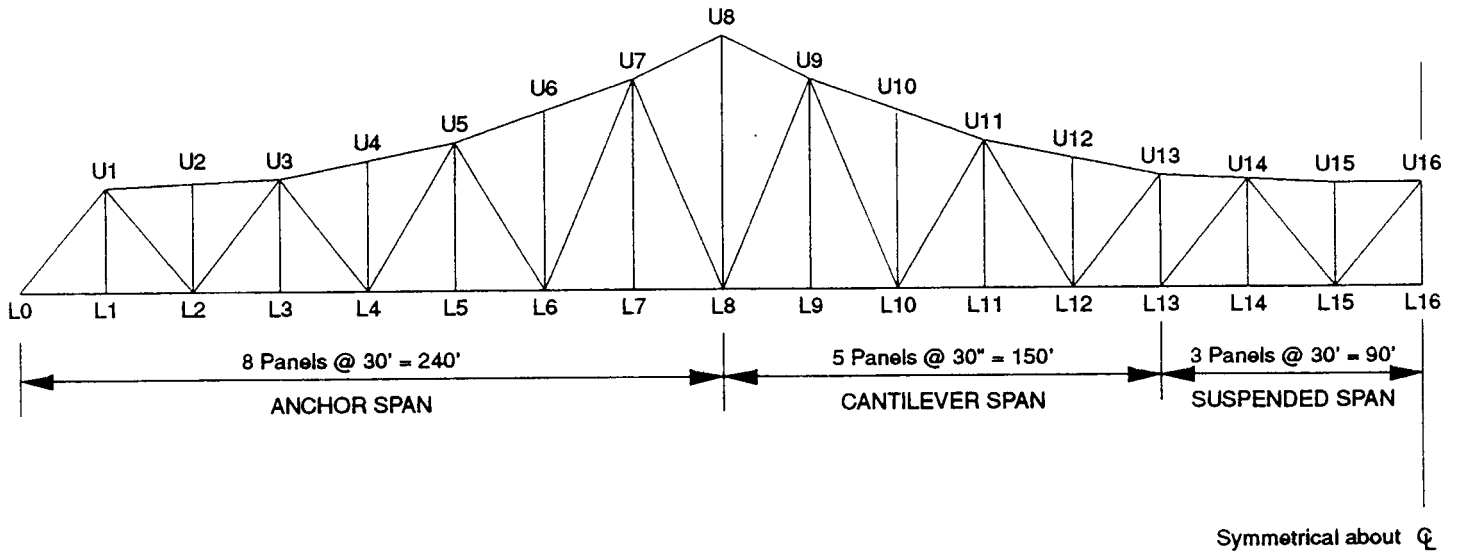


Figure 7. I-270 over Chain-of-Rocks Canal. Bridge is symmetrical about the centerline.

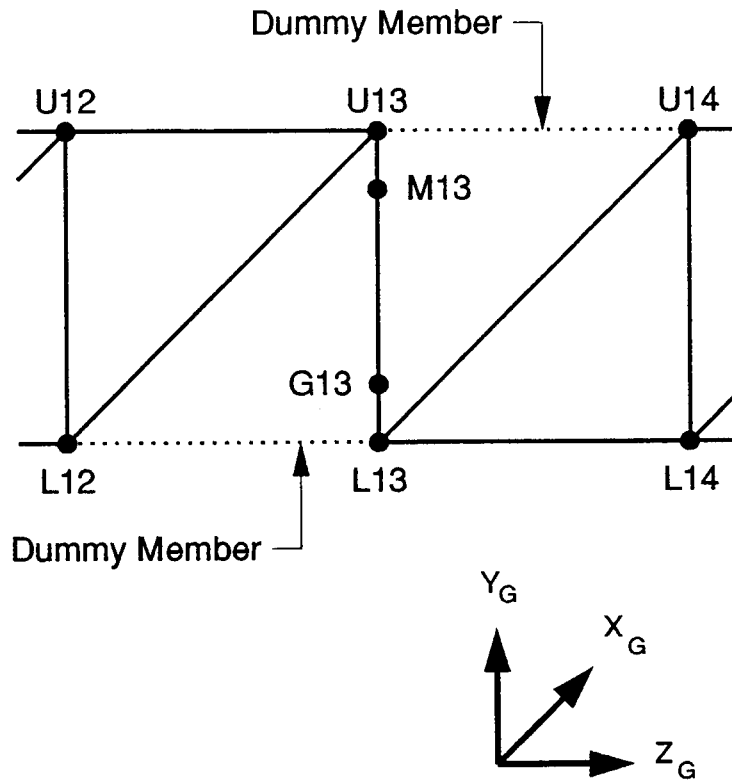


Figure 8. Finite element approximation of a truss section near a hanger on I-270 over Chain-of-Rocks Canal. Pins are located at nodes M13 and G13.

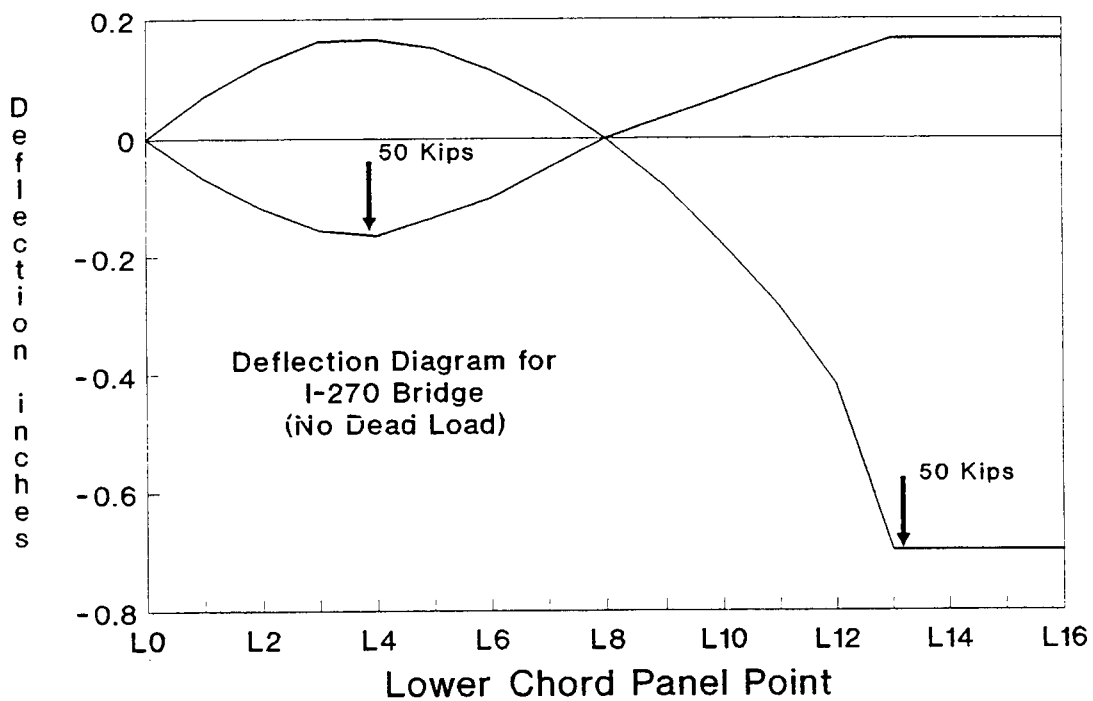


Figure 9. Static deflection diagram of lower chord of I-270 bridge, without deadload effect.

$$\tau_t = \frac{Tr}{J} \quad (1)$$

Where τ_t = Torsional shear stress on pin (ksi)
 T = Torque on pin (kip-inches)
 r = Radius of pin (inches)
 J = Polar area moment of inertia (inches⁴)
= $\frac{\pi d^4}{32}$ where d = diameter of pin (inches)

Torques and resulting torsional shear stress for this bridge are shown in Table 1. The torque data generated was compared to a simplified calculation based on angles developed using slope-deflection methods. The difference between the average of the finite element data and the simplified calculation was 5.7%.

TABLE 1

TORQUE AND TORSIONAL SHEAR STRESS ON SEVEN-INCH
DIAMETER PINS (I-270) COMPLETELY FIXED

<u>PIN DESIGNATION</u>	<u>TORQUE (KIP-IN)</u>	<u>TORSIONAL SHEAR STRESS (KSI)</u>
M13 (Upper)	2102	31
N13 (Upper)	2103	31
G13 (Lower)	2218	33
H13 (Lower)	2218	33

Using distortion energy yield criteria the yield strength in shear is given by:

$$S_{SY} = 0.667S_Y \quad (2)$$

Where S_{SY} = Yield strength in shear (ksi)

S_Y = Yield strength in tension (ksi).

The tensile yield strength for ASTM A237-A is 50 ksi. Therefore, the shear yield strength for these pins is 33 ksi. As indicated in Table 1 above, completely fixed pins on this bridge, subjected to a thermal differential of 50°F, experience shear stresses equal to or very close to the shear yield strength, even without considering ambient shear stress in the pins resulting from dead load, live load, and impact. Ambient shear stress in the pins for this bridge based on dead load, live load, and impact are on the order of 6 ksi. It should be noted here that the completely fixed pin joint used in the computer model (equivalent to a frame connection) allows absolutely no rotation.

I-474 Over Illinois River

The truss section of this bridge is 1,140 feet long. The cantilevered span is 150 feet long, and the suspended span is 240 feet long. The structure was built circa 1970. This structure was computer-modeled similarly to the previous I-270 bridge analysis. Marked physical differences, in addition to respective span lengths and the resulting differences in sectional properties, between this and the I-270 bridge include total width (45'-3" center to center of trusses versus 38'-0" for I-270), increased use of welded members on I-474, especially on the suspended span, and use of K-bracing for the upper and lower lateral bracing on I-474 as opposed to X-bracing on I-270. These differences do not materially affect the gross structural behavior of the respective bridges and are mentioned only in order to note that the two bridges are dissimilar in other ways besides length. The most significant difference from a pin fixity standpoint was the use of a full length sleeve to cover the pins on I-474. Modeling and checking methods

were similar for both bridges. Pin torques and shear stresses are shown in Table 2.

The pins on the I-474 bridge are twelve-inch diameter, AASHTO Specification M 192 Class 120. The minimum specified yield strength of this material is 95 ksi. The resulting shear yield strength, S_{SY} , from (2) is 63 ksi.

TABLE 2

TORQUE AND TORSIONAL SHEAR STRESS ON TWELVE-INCH
DIAMETER PINS (I-474) COMPLETELY FIXED

<u>PIN DESIGNATION</u>	<u>TORQUE (KIP-IN)</u>	<u>TORSIONAL SHEAR STRESS (KSI)</u>
M15 (Upper)	4705	14
N15 (Upper)	4703	14
G15 (Lower)	4949	15
H15 (Lower)	4946	15

Comparison of torsional shear stress from Table 2 and the shear yield strength shows that the pins on the I-474 bridge are nowhere near failure due to complete fixity and a 50°F temperature change. The primary dimensional variables relating to the calculated torsional shear stresses are cantilever length, suspended span length, hanger length between pins, and pin diameter. The first three contribute to the torque being applied. Pin diameter specifies radius and polar moment of inertia in (1). The other important variables are temperature change and pin material.

Hazel Dell Road Over I-55 at Springfield

This structure is a five-span, multi-stringer bridge approximately 330 feet long. The two side spans are cantilevered from the end piers.

The suspended portions span from the abutments to the ends of the cantilevers. See Figure 10. Thermal movement is accommodated with expansion joints in the side spans at the ends of the cantilevers. The suspended portions are supported using pin-link eyebar connections. The pins are three inches in diameter and are three inches long between each shoulder. Total pin length, including threads, is 5.75 inches. This bridge was modeled completely since some asymmetries exist. Stringers are on 5'-9" spacings. The pins were simulated as with the previous truss bridges. This model was checked for geometry, static deflection, and thermal expansion. The maximum torque produced by a 50°F temperature differential was 50.4 kip-inches. The resulting torsional shear stress is 9.5 ksi. Ambient pin shear stresses due to dead load and live load are on the order of 1.5 ksi. However, when the torque induced in fixed pins due to live load is considered, the maximum torque is 767.5 kip-inches and the maximum shear stress on the pins is 144.8 ksi, assuming completely elastic behavior. The pin material was ASTM A36 steel with a shear yield strength of 24 ksi. The pin is by calculation clearly yielded. A completely fixed condition for these pins results in permanent deformation and possible rupture. Even though the computer model represents worst case conditions, very high shear stresses may be assumed to be induced in pins which are becoming fixed due to corrosion.

Stresses In Hangers and Link Eyebars

The major focus of this investigation was on pins. However, the potential for failure of the hangers or link eyebars due to fixity-induced loadings was also investigated. Fixity induces stresses into connecting members which are not considered in design assumptions.

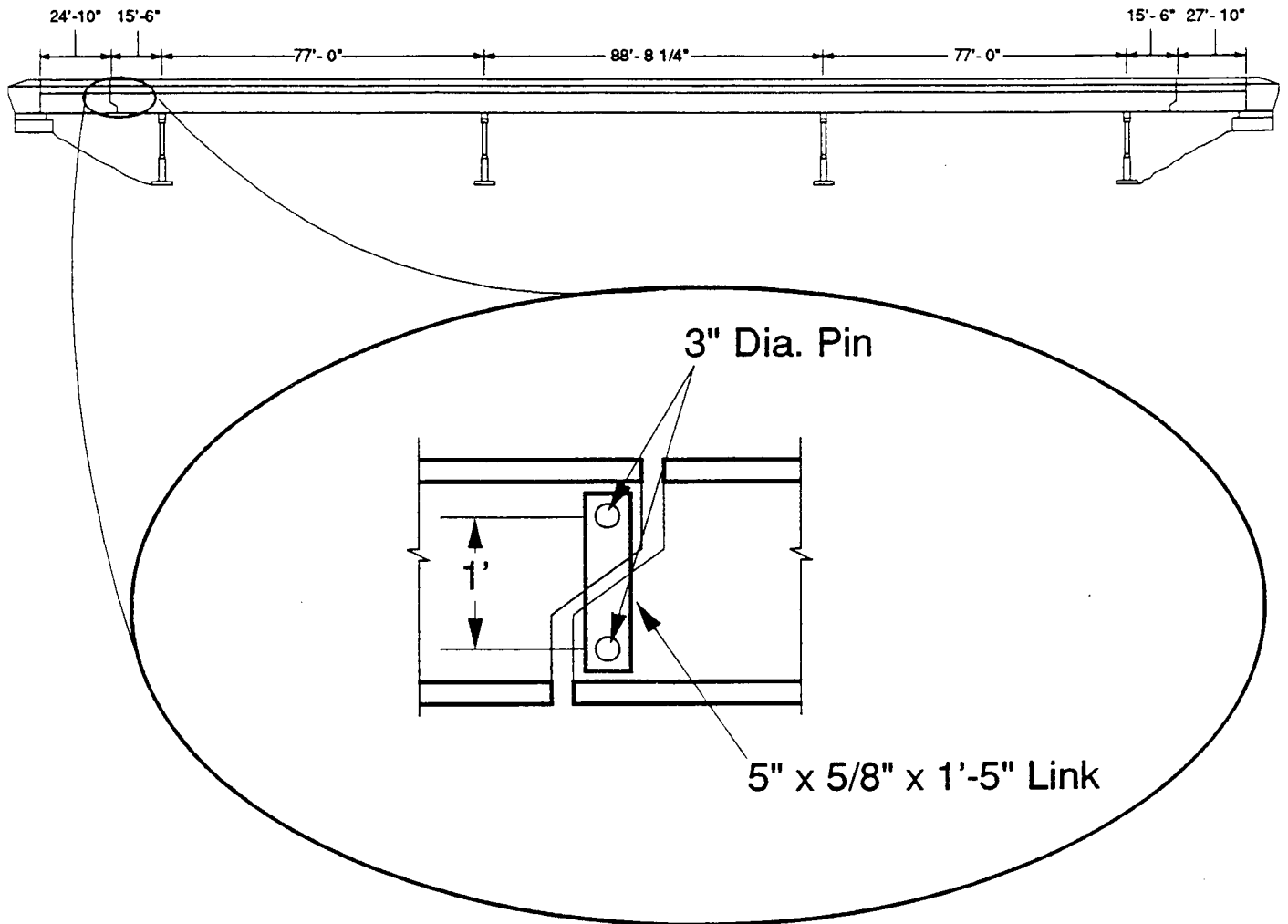


Figure 10. Hazel Dell Road over I-55 in Springfield, Illinois.

Ambient hanger tensile stresses due to dead load, live load, and impact, based on loads given in the design plans for the two cantilever truss bridges studied were on the order of 16 ksi. The torque moment induced by fixity also induces bending stresses in the hanger members. These stresses were on the order of 14 ksi at the nominal section of the hanger. The combination of these stresses approaches the yield strength for mild (ASTM A36) steel, and could be further increased by the existence of various stress concentrations such as surface pitting, wear scores, or notches. Fatigue damage of the components could also be a concern, even for members which are not completely fixed. Large temperature changes, especially common in spring and fall, would produce daily cyclic loadings sufficient to produce cumulative damage. This fatigue aspect should be studied in more detail.

The link eyebars on cantilever girder bridges can develop high stresses, especially near the pin holes. Ambient axial stresses in the link eyebars due to dead load and live load, based on finite element data, were on the order of 7 ksi for free pins. Considering the stress concentration factor for a plate loaded in tension by a pin through a hole, with clearance,³ to be 3.6, this results in a peak stress of 25 ksi. This stress level is even higher when fixity is considered. Using the data generated by the finite element model, the shear stress on the links induced by live load with fixed pins is on the order of 31 ksi at the outer periphery of the link eyebar, near the pin. Thus, both link eyebars and pins are in jeopardy when complete fixity is present in the detail. Again, these numbers were generated for the detail in a completely fixed condition. Fixity, or even partial fixity, in pin-link eyebar details is a serious condition and should be scheduled for quick repair using a retrofit detail which will alleviate the problem, not just postpone it.

4. EXPERIMENTAL STRESS ANALYSIS

Instrumentation and stress analysis using strain gages on large pin connections in cantilever truss bridges is discussed in this chapter.

The basic configuration of the instrumented location was shown in Figure 4. The Wheatstone bridge circuit relevant to this application is shown in Figure 11. Using the notation shown in Figure 11, let ϵ_B be the bending strain due to the applied moment M (due to fixity) and let ϵ_P be the axial strain due to dead load, live load and thermal effects. The basic rule of the Wheatstone bridge is that adjacent arms subtract and opposite arms add (algebraically). The output from Gages 1 and 3 is $\epsilon_B + \epsilon_P$ each. The output from Gages 2 and 4 is $-\epsilon_B + \epsilon_P$ each. The output from the total circuit is Gage 1 - Gage 2 + Gage 3 - Gage 4. Therefore,

$$\text{OUTPUT} = 4 \epsilon_B \quad (3)$$

$$\text{or,} \quad \epsilon_B = \text{OUTPUT}/4 \quad (4)$$

Where OUTPUT is the reading given by the strain gage indicator. This circuit, therefore, provides high sensitivity to bending, thermal compensation, and insensitivity to axial load effects. The only strains measured by this installation are due to bending.

The bending stress is then calculated from

$$\sigma_B = E \epsilon_B \quad (5)$$

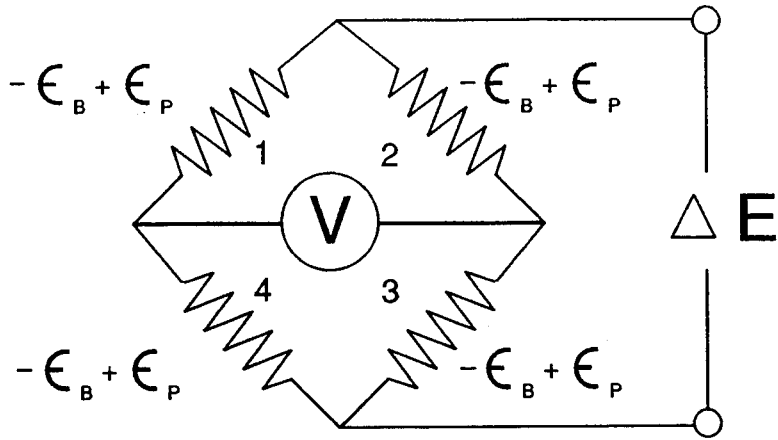


Figure 11. Wheatstone bridge circuit diagram for measurement of bending strains with insensitivity to axial strains.

Where E is the elastic modulus for steel.

The bending moment is calculated from:

$$M = \frac{\sigma_B I}{c} \quad (6)$$

Where M = Bending moment (kip-in)

σ_B = Bending stress (ksi) calculated from strain gage data.

I = moment of inertia of instrumented section about the appropriate axis (inches⁴).

c = distance from the centroid of the instrumented section to the outer fiber (strain gage thickness is ignored) (inches).

This bending moment is then used as torque T in (1) to calculate the torsional shear stress on the pin.

The procedure used for data collection was to collect initial reference strain and surface temperature data, then collect strain and temperature data at a later date. From these data temperature differential and bending strain are calculated. The strain gages used were weldable, electrical resistance foil strain gages manufactured by MicroMeasurements of Raleigh, North Carolina. The strain gage indicator was also manufactured by MicroMeasurements.

Tables 3 and 4 present data collected and analyzed for the I-270 and I-474 bridges, respectively. Only lower pins were instrumented.

TABLE 3

STRAIN GAGE DATA AND ANALYSIS FOR
I-270 BRIDGE

GAGE LOCATION*	Temperature	Strain	Stress in hanger	Moment	Torsional stress (shear)
	ΔT (Deg F)	ϵ_B (10^{-6} in/in)	σ_B (ksi)	M (kip-in)	T_t (ksi)
EB-W-U	51	101.25	3.0375	718.34	10.67
EB-E-U	INSTALLATION DESTROYED				
WB-W-D	INSTALLATION DESTROYED				
WB-E-D	INSTALLATION DESTROYED				
WB-W-U	42	31.0	0.93	219.94	3.27
WB-E-U	64	87.5	2.63	620.79	9.22

TABLE 4

STRAIN GAGE DATA AND ANALYSIS FOR
I-474 BRIDGE

GAGE LOCATION*	Temperature	Strain	Stress in hanger	Moment	Torsional stress (shear)
	ΔT (Deg F)	ϵ_B (10^{-6} in/in)	σ_B (ksi)	M (kip-in)	T_t (ksi)
WB-E-U	21	33.75	1.01	394.27	1.16
WB-W-U	22	11.75	0.35	136.63	0.40
WB-E-D	INSTALLATION DESTROYED				
WB-W-D	21	21.75	0.65	253.74	0.75

*For example, EB-W-U stands for eastbound, westside, upstream.

The total shear stress, τ_T , is then

$$\tau_T = \tau_a + \tau_t \quad (8)$$

Where τ_a = ambient shear stress from dead load, live load and impact.

τ_t = torsional shear stress in pin due to fixity effects.

The total shear stress may then be compared to the shear yield strength of the material, given by (2).

In Chapters 3 and 4, two separate, important methods of analysis were discussed. Finite element analysis was used to estimate the maximum effect of complete fixity on pin connection details. This type of analysis could indicate whether complete pin fixity in a particular bridge is a serious potential problem or not. In NCHRP Report 333, Kulicki, et al,⁴ suggest a hand calculation method for evaluating the magnitude of the bending moments induced in a hanger due to completely fixed pins. This method could be useful in the absence of a finite element analysis for establishing the level of shear stress in pins due to fixity for cantilever truss bridges. The experimental stress analysis is needed to actually determine the torsional shear stresses induced in pins due to an unknown degree of fixity. These stresses, combined with the ambient shear stress calculated from design loads, may be compared to the shear yield strength for a given pin material, as shown above.

5. ULTRASONIC PIN INSPECTION

This chapter discusses the development of an ultrasonic pin inspection procedure, results and unit costs of two pilot inspection contracts, overall results, and comparison of ultrasonic test techniques to detect defects in the form of machined notches of known depth.

There are many pin-and-link eyebar configurations in use in Illinois bridges. This variety comes from the fact that consultant designers were given wide latitude to provide a detail which would satisfy design stress criteria. As a result, pins vary by diameter, length (both total and threaded), shoulder depth, and retaining method. This wide variation of pin geometry requires a very flexible pin inspection procedure. Ultrasonic testing was chosen as the principal inspection method because visual inspection and magnetic particle methods provide limited information, and both acoustic emission and radiographic testing are costly and time consuming.

Development of Procedure

It was decided very early in the project that the inspection procedure must be sufficient to provide nearly 100% coverage of the load bearing portion of the pin from the pin face. In order to accomplish this, two scanning methods were included in the procedure. Longitudinal, or straight beam scanning, is used for detection of flaws such as large cracks or wear grooves. Angle beam, or shear wave scanning, is used to provide additional coverage of the pin during inspection. Wedge angle selection is typically 20, 30, or 45 degrees. Angle beam testing can generally detect small defects that cannot be detected during straight beam testing due to shoulder depth. A 3.5 MHz, 1/2-inch diameter

quick-change transducer was selected to provide a combination of sensitivity, depth of penetration, and low beam divergence.

No available standard reference block had features that would allow calibration of a 20 degree wedge, so a suitable reference block was developed. The Distance and Sensitivity Calibration - Pin (DSC-P) calibration block was fabricated by in-house machinists for calibrating straight beam transducers and the 20, 30, and 45 degree wedges to a 0.06-inch diameter hole. The DSC-P block is shown in Figure 12.

The Reference Levels for straight and angle beam testing are the gain setting needed to bring the 0.06-inch diameter hole in the DSC-P calibration block to 50% screen height. When calibrating for sensitivity, the sound path for shear wave testing was the same as that used for straight beam. Scanning level is typically 18-20 dB above the Reference Level. The complete procedure, including data recording sheets, is given in Appendix A.

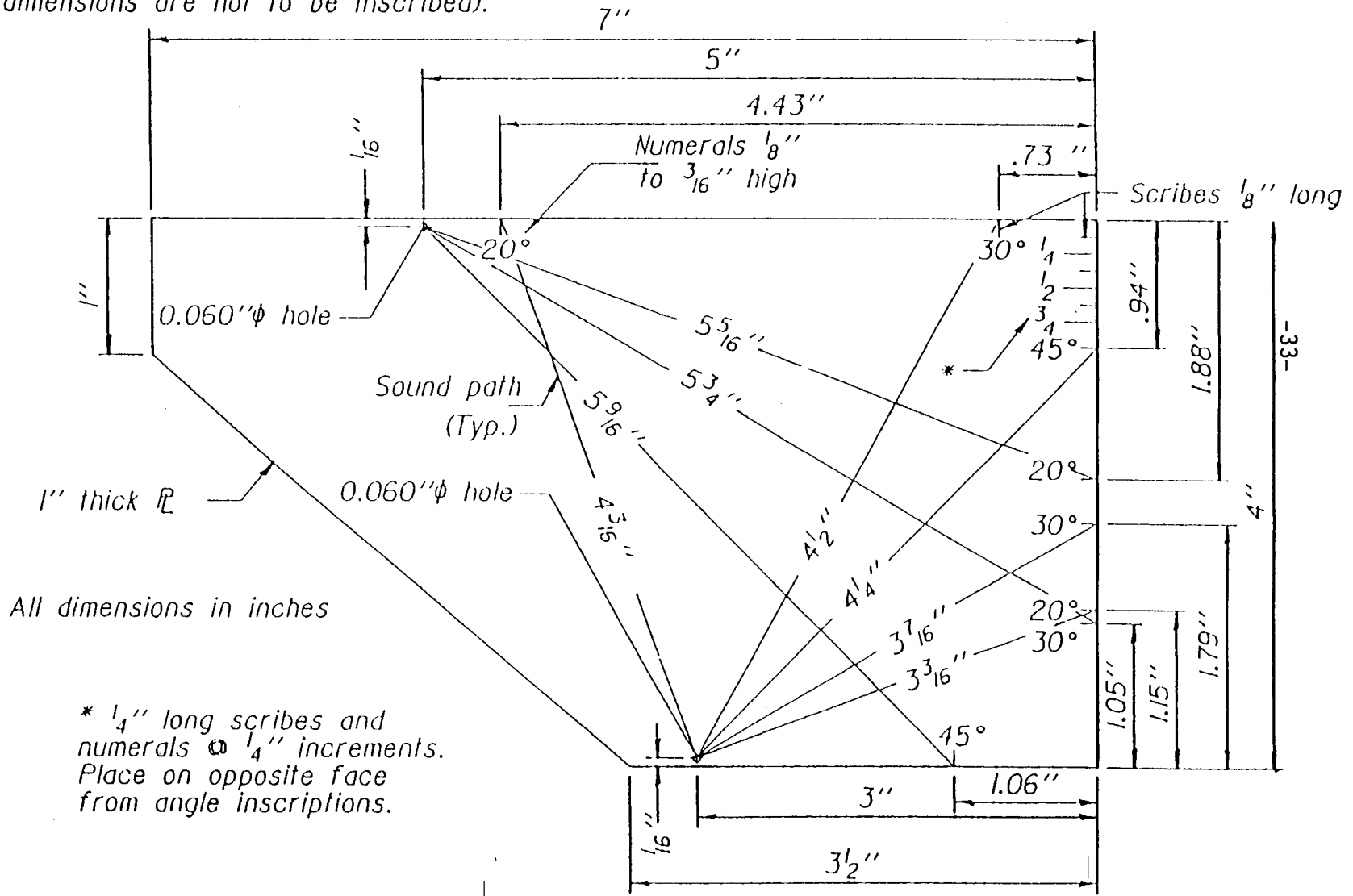
Pin Inspection Contracts

Two pilot contracts were let for initial ultrasonic pin testing of all state-maintained cantilever girder bridges. These contracts were conducted in the summers of 1989 and 1990. A different consultant was used for each contract. Inspectors were required to be certified as Level II UT inspectors. All access and traffic control was supplied by the Department. Each consultant was provided with a DSC-P calibration block and detailed drawings showing pin cross sections.

Notes:

1. The dimensional tolerance between all surfaces involved in referencing or calibrating shall be within ± 0.005 in (.13 mm) of detailed dimension.
2. The finish of all faces to which sound is applied or reflected from shall have a maximum ANSI surface roughness of 125μ in (r.m.s.)
3. All material shall be AISI 1018 or acoustically equivalent, with no detectible internal defects @ 80 dB setting with a $\frac{1}{2}$ " ϕ , 3.5 MHz, straight beam transducer.
4. All holes shall have a smooth internal finish and shall be drilled at 90 degrees to the material surface.
5. Degree lines and identification markings shall be indented into the material surface so that permanent orientation can be maintained. (Sound paths and dimensions are not to be inscribed).

Figure 12. Distance and Sensitivity Calibration-Pin (DSC-P) calibration block developed for use with pin inspections.



* $\frac{1}{4}$ " long scribes and numerals @ $\frac{1}{4}$ " increments. Place on opposite face from angle inscriptions.

IL DOT DSC - P* test block
* Distance & Sensitivity Calibration - Pin

1989 Inspection Contract

The inspections started on August 3, 1989 and ended on October 5, 1989. The department provided surface preparation of the pin faces. All paint, rust, and debris was removed by small grinding tools. The inspectors used a plain center punch to identify the twelve o'clock position on the A face (see Appendix A) of all pins to provide a consistent reference point for future inspections.

Forty-four structures containing 813 pins were inspected during this contract. Department personnel evaluated all inspection reports and placed sixteen structures on a two year inspection frequency. The inspection frequency was roughly correlated to a condition rating assigned to each structure based upon the Indication Ratings of the pins.

The lowest recorded Indication Rating was - 4dB on one pin in a structure with multi-girder, single pin, suspended spans. This indicates that 4dB less gain was needed to bring the indication to 50% screen height compared to the reference signal. On removal, it was apparent that wear grooves in the pin of approximately 3/8-inch were the cause of the low Indication Rating. The original pin diameter was 2-1/2 inches. See Figure 13.

Problems were encountered in testing link pins with nut-retaining cotter pins in each end. The interference from the drilled hole hampered testing, especially with the angle beam transducer. The consultant believed some pins could not be tested due to severe scattering of the sound beam due to the pin alloy or its heat treatment, such as carburizing.

The consultant's final report included a summary of procedures used, modifications to the procedures developed by the Department and

recommendations for improving the procedures, a summary of structure numbers and locations where defects were found and the Indication Rating of the defects, and a special summary of any significant defects found.

1990 Inspection Contract

The inspections started on June 20 and ended on October 25, 1990. A drawing was required of each structure in plan view showing how the consultant labeled each girder and pin so the layout could be duplicated for future inspections. The consultant was also required to document the method of access to the pins.

The consultant was instructed to assign a subjective fracture critical appraisal rating to each structure based on the assessment of the overall condition of the pins. The rating is an arbitrary number from 0-8 derived from the ultrasonic measurements which indicates the overall condition of a fracture critical member. See Appendix B. The consultant was inspecting two types of fracture critical structures; Multi Girder System - Suspension Links and Pins, Code G1, and Multi Girder Systems Suspension Single Pins, Code G2. The 1989 consultant inspected the same structure types but was not required to assign the ratings. Eighty-six structures were inspected under this contract.

The consultant assigned a fracture critical rating of 0-8 to each structure. A rating of 6 or less placed the structure on a two-year ultrasonic inspection frequency. A rating of 7 or 8 placed the structure on a five-year ultrasonic inspection frequency. Forty-two of the eighty-six structures were given an appraisal rating of 6 or less and were placed on a two-year inspection frequency.

To improve calibration the consultant recommended a model be made with the same material and geometry as each in-service pin. The model

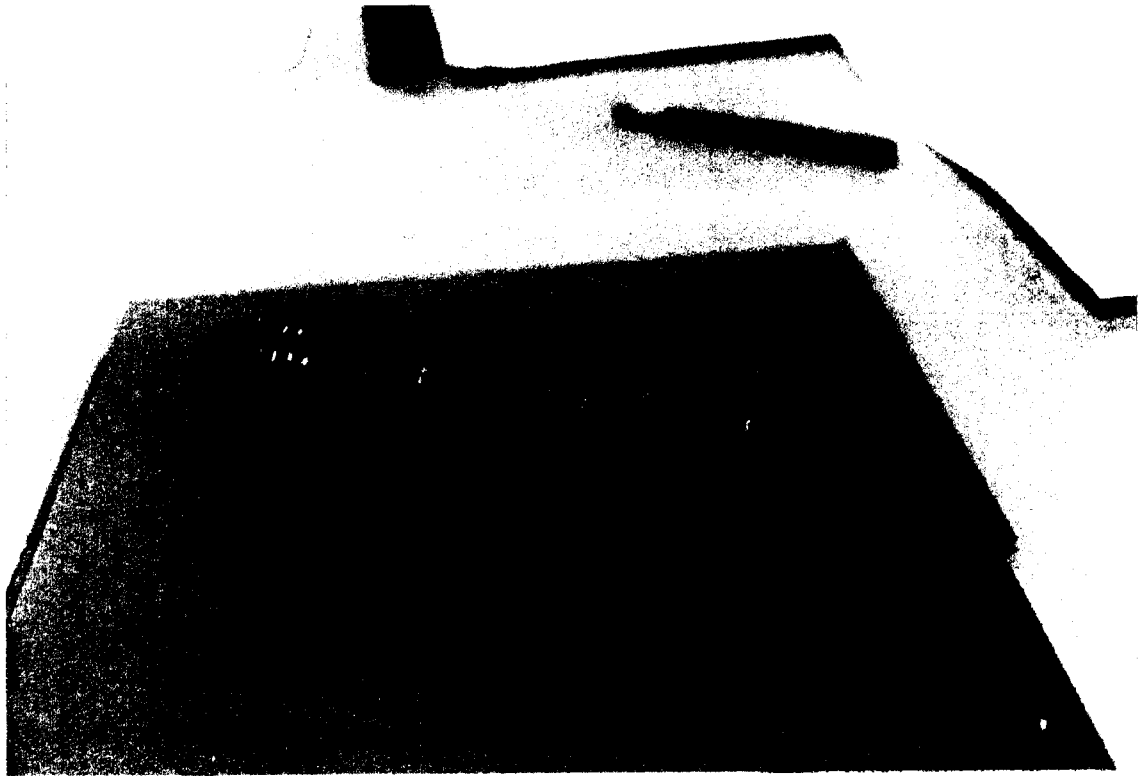


Figure 13. Photograph of pin with deep wear grooves.

should contain a flaw that would allow a pass-reject test instead of determining Indication Ratings. An analysis of this notched pin vs. dB indication can be found on page 38.

Overall Results

A total of 130 structures containing 3,165 pins were inspected at a unit cost of \$73.60 per pin. This unit cost includes both consultant and indirect labor and equipment costs to the state. Table 5 shows the distribution of structures with fracture critical appraisal ratings ranging from zero to eight. The resulting inspection frequencies are also shown.

TABLE 5

DISTRIBUTION OF STRUCTURES WITH FRACTURE
CRITICAL APPRAISAL RATINGS OF 0-8

Appraisal Rating	8	7	6	5	4	3	2	1	0
No. of Structures	23	50	39	11	5	2	0	0	0
Inspection Frequency, yrs	5	5	2	2	1	1	-	-	-

Nearly all structures were inspected in one or two working days. A couple of large structures required up to four working days.

Based on the experience with these two pilot contracts, some changes were made in the inspection procedure. These changes included deleting an adjustment factor based on shoulder depth and use of a reference pin for each individual bridge. The adjustment factor was deleted because it increases the gain level used for scanning and resulted in too much background noise, which is often referred to as oscilloscope "grass". This background noise often obscured the real defect. In response to future

testing requirements, IDOT created an in-house ultrasonic testing unit within its Bureau of Bridges and Structures. To provide for a better inspection program, a library of pins and plans for each structure in the state with pin details is being developed. This library will allow the inspector to carry a pin of the same geometry with known defects to a specific bridge and compare inspection results to the reference pin. The procedure still uses a round hole to calibrate for a groove or crack.

No pins were found to have large cracks or sustain complete fractures. Large cracks or partial fractures are immediately apparent on the instrument CRT screen as shown by the loss or reduction of back echo from the opposite pin end. Many carburized pins, even those installed as recently as two years ago, tend to have more severe Indication Ratings than many in-service untreated pins. These ratings are attributed quench microcracks in the pin surface and the difference in sound transmission in high carbon vs. low carbon steel. From an ultrasonic inspection viewpoint, continued use of carburized pins is not recommended due to the severity and number of indications.

Comparison of Defect Size with Test Results

A testing program was conducted to try to relate ultrasonic inspection results to defects of known size and location. The testing program included straight-beam, 20-, 30-, and 45-degree shear beams. The transducer frequency was 3.5 MHz. Two specimen types were used. One was an actual pin removed from a bridge. This three-inch diameter pin had a 3/8-inch shoulder, 1.25-inch threaded length on both sides, and was 7.25 inches long. The surface of the pin was slightly pitted, and had very shallow (about 1/32-inch) wear grooves. The pin material is unknown, but was assumed to be ASTM A36 steel. The other specimen was a longitudinal

cross-section of the same pin geometry. Two of these specimens were fabricated from 3/4-inch ASTM A572 steel plate.

The defect used in this testing program was a 1/16-inch nominal width saw-cut notch which had varying depth and spacing. For the pin specimen, the notch depths used were 1/16-, 1/8-, 1/4-, and 1/2-inch. By judicious placement of the notches, several sound path distances for each notch were achieved. For the plate specimens, the notch depths were 1/16-, 1/8-, 1/4-, and 3/8-inch. Each side of each specimen had a constant notch depth. Seven notches were placed at 1/2-inch spacings beginning two inches from the side of the specimens.

The collected data were analyzed for three cases: 1) use of unadjusted data only, 2) use of the IDOT developed pin inspection procedure, and 3) use of the developed pin inspection procedure but without application of the distance attenuation correction factor. Tables 6 and 7 show average and standard deviation for each case for the pin and the plate specimens, respectively. These data were also plotted as shown in Figures 14 through 21. The plots show the data scatter in the form of error bands. The size of each error band is plus and minus one standard deviation from the average.

The following observations are made from the data:

- 1) In almost every case, the difference between the inspection procedure with and without distance attenuation is very small. This suggests that the distance attenuation correction factor is not really needed.
- 2) The longitudinal beam data show a reasonable variation with notch depth, especially for the data from the pin specimen. The longitudinal beam data from the plate specimen show an inability to differentiate between 1/16- and 1/8-inch notches.

TABLE 6

ULTRASONIC DATA FOR NOTCHES OF KNOWN
DEPTH AND LOCATION IN AN ACTUAL PIN*

TRANSDUCER	NOTCH DEPTH (INCHES)							
	0.0625"		0.125"		0.250"		0.500"	
	<u>db</u>	<u>std dev</u>	<u>db</u>	<u>std dev</u>	<u>db</u>	<u>std dev</u>	<u>db</u>	<u>std dev</u>
Long. Beam	73.5	(3.2) Unadjusted data	60.0	(4.1)	54.0	(4.7)	42.5	(5.3)
	22.8	(5.2) IDOT procedure	9.3	(3.6)	3.4	(2.8)	-8.3	(8.4)
	21.5	(3.2) IDOT w/o Dist.	8.0	(4.1)	2.0	(4.7)	-9.5	(5.3)
20-deg.	63.5	(1.9) Unadjusted data	64.3	(4.6)	69.3	(5.6)		N/O
	-15.8	(1.8) IDOT procedure	-18.6	(3.9)	-11.0	(5.8)		N/O
	-14.5	(1.9) IDOT w/o Dist.	-17.7	(3.9)	-10.7	(5.3)		N/O
30-deg.	63.0	(4.8) Unadjusted data	55.0	(1.4)	52.0	(0)	53.0	(1.4)
	-14.4	(5.0) IDOT procedure	-22.6	(1.4)	-25.6	(0)	-24.6	(1.4)
	-13.0	(4.8) IDOT w/o Dist.	-21.0	(1.4)	-24.0	(0)	-21.0	(1.4)
45-deg.	59.0	(2.6) Unadjusted data	54.0	(5.7)	52.0	(1.4)		N/O
	-24.8	(2.8) IDOT procedure	-30.1	(5.7)	-32.1	(2.8)		N/O
	-23.0	(2.6) IDOT w/o Dist.	-28.0	(5.7)	-31.0	(4.2)		N/O

*Data shown are averages for varying numbers of collected data points.

N/O = not obtainable due to geometry of that specimen.

TABLE 7

ULTRASONIC DATA FOR NOTCHES OF KNOWN DEPTH
AND LOCATION IN PLATE SPECIMENS*

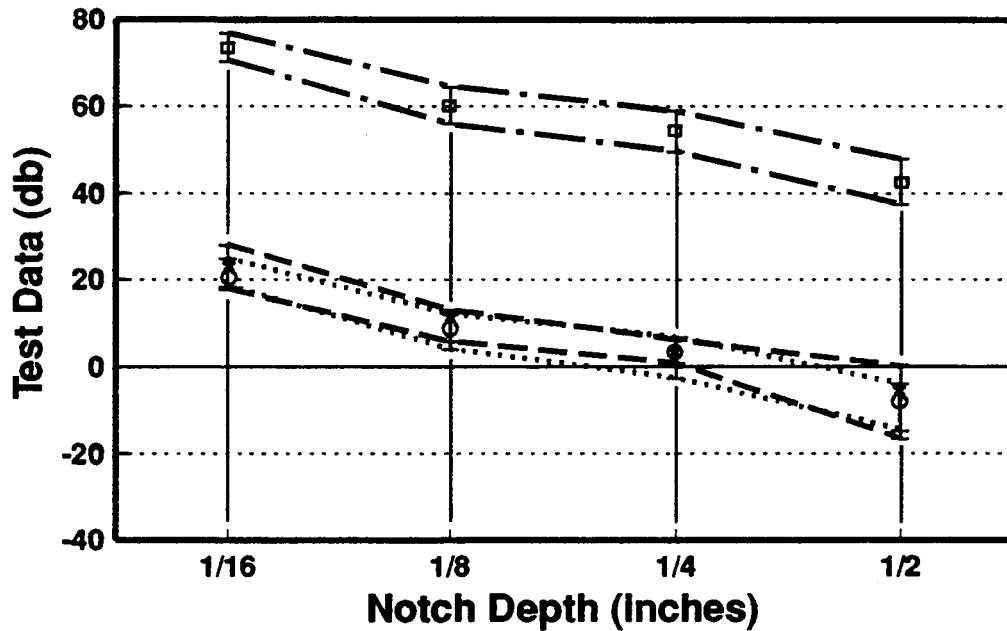
TRANSDUCER	NOTCH DEPTH (INCHES)									
	0.0625"		0.125"		0.250"		0.375"			
	<u>db</u>	<u>std dev</u>	<u>db</u>	<u>std dev</u>	<u>db</u>	<u>std dev</u>	<u>db</u>	<u>std dev</u>	<u>db</u>	<u>std dev</u>
Long. Beam	72.50(2.2)	Unadjusted data	72.0 (3.3)		65.4 (3.0)		59.4 (4.3)			
	21.1 (1.8)	IDOT procedure	21.1 (3.5)		14.7 (3.0)		8.7 (5.8)			
	19.9 (2.3)	IDOT w/o Dist.	19.9 (3.5)		13.4 (3.0)		7.4 (4.3)			
20-deg.	71.2 (5.0)	Unadjusted data	61.6 (4.3)		63.0 (8.1)		58.3 (5.3)			
	-10.5 (7.4)	IDOT procedure	-20.0 (9.7)		-20.3 (9.6)		-23.2 (6.7)			
	-10.5 (7.4)	IDOT w/o Dist.	-20.4 (5.1)		-19.0 (10.9)		-23.1 (6.8)			
30-deg.	63.4 (2.7)	Unadjusted data	69.1 (9.1)		66.2 (5.0)		77.7 (2.1)			
	-13.9 (3.0)	IDOT procedure	-8.2 (3.9)		-11.1 (4.8)		0.6 (3.1)			
	-13.4 (2.1)	IDOT w/o Dist.	-7.6 (4.6)		-10.4 (5.5)		1.4 (2.5)			
45-deg.	79.3 (1.2)	Unadjusted data	75.0 (4.2)		57.5 (5.3)		78.0 (2.8)			
	- 4.9 (1.4)	IDOT procedure	-9.6 (3.8)		-26.9 (4.7)		-7.2 (3.2)			
	- 2.7 (1.2)	IDOT w/o Dist.	-7.0 (4.2)		-24.5 (5.3)		-4.0 (2.8)			

*Data shown are averages for varying numbers of collected data points.

- 3) The angle beam data do not show any reasonable relations to notch depth. The data are widely scattered and show large statistical variation.

Further work is needed to establish a correlation between inspection results and actual defect size. Such work should include higher frequencies, compression wave transducers, and other defect shapes. More work is also needed to develop an adequate procedure to inspect link eyebars and link plates for cracks.

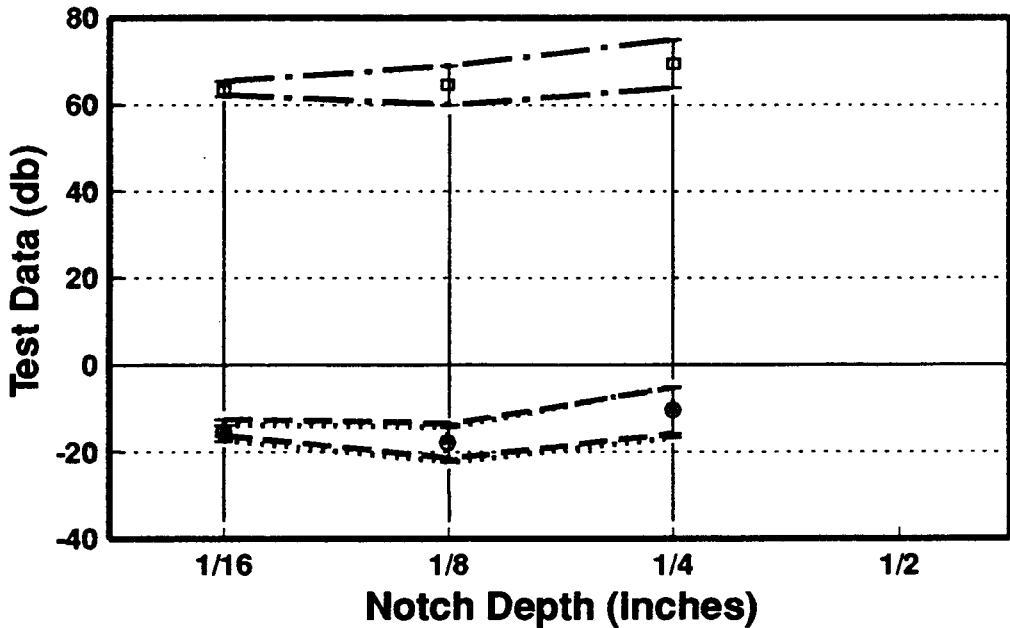
Ultrasonic Data For Actual Pin Specimen Straight Beam Transducer f=3.5MHz



- db Level Required To Put Signal At 50% Screen Height (No Distance or Reference Compensation)
 - *--- IDOT Procedure
 - ...○... IDOT Procedure Without Distance Attenuation Correction Factor
- Bands Show +/- 1 Std Dev. From Average

Figure 14. Ultrasonic test data for an actual 3-inch diameter pin specimen using a straight beam transducer. Figure shows unadjusted data, results from IDOT procedure, and results from IDOT procedure without distance attenuation correction factor.

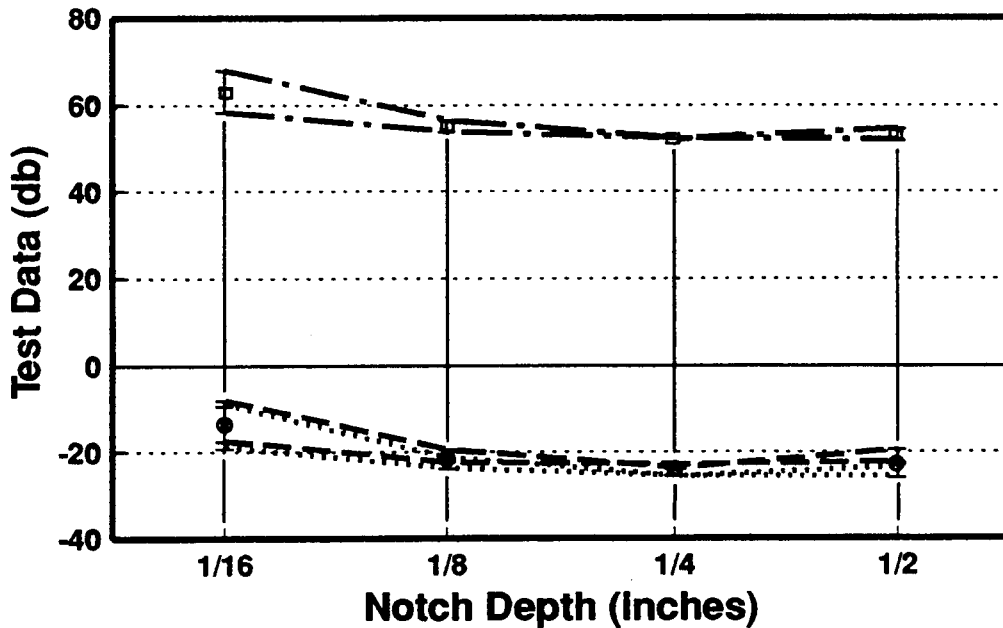
Ultrasonic Data For Actual Pin Specimen 20 Degree Angle Beam Transducer f=3.5MHz



- db Level Required To Put Signal At 50% Screen Height (No Distance or Reference Compensation)
 - * IDOT Procedure
 - IDOT Procedure Without Distance Attenuation Correction Factor
- Bands Show +/- 1 Std Dev. From Average

Figure 15. Ultrasonic test data for an actual 3-inch diameter pin specimen using a 20 degree angle beam transducer. Figure shows unadjusted data, results from IDOT procedure, and results from IDOT procedure without distance attenuation correction factor.

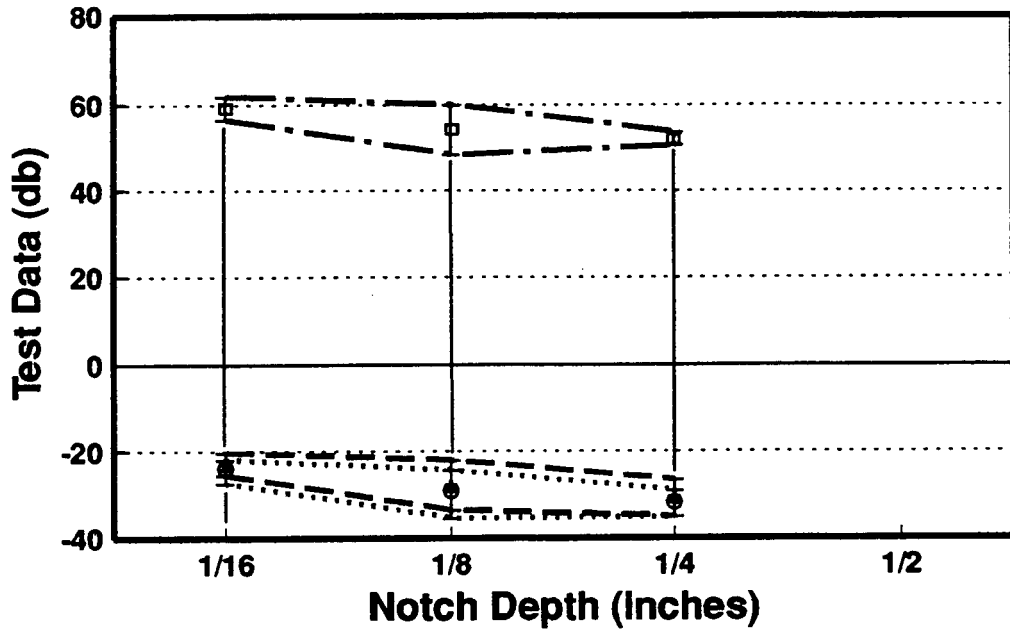
Ultrasonic Data For Actual Pin Specimen 30 Degree Angle Beam Transducer f=3.5MHz



-  db Level Required To Put Signal At 50% Screen Height (No Distance or Reference Compensation)
 -  IDOT Procedure
 -  IDOT Procedure Without Distance Attenuation Correction Factor
- Bands Show +/- 1 Std Dev. From Average

Figure 16. Ultrasonic test data for an actual 3-inch diameter pin specimen using a 30 degree angle beam transducer. Figure shows unadjusted data, results from IDOT procedure, and results from IDOT procedure without distance attenuation correction factor.

Ultrasonic Data For Actual Pin Specimen 45 Degree Angle Beam Transducer f=3.5MHz



---□--- db Level Required To Put Signal At
50% Screen Height (No Distance or Reference Compensation)

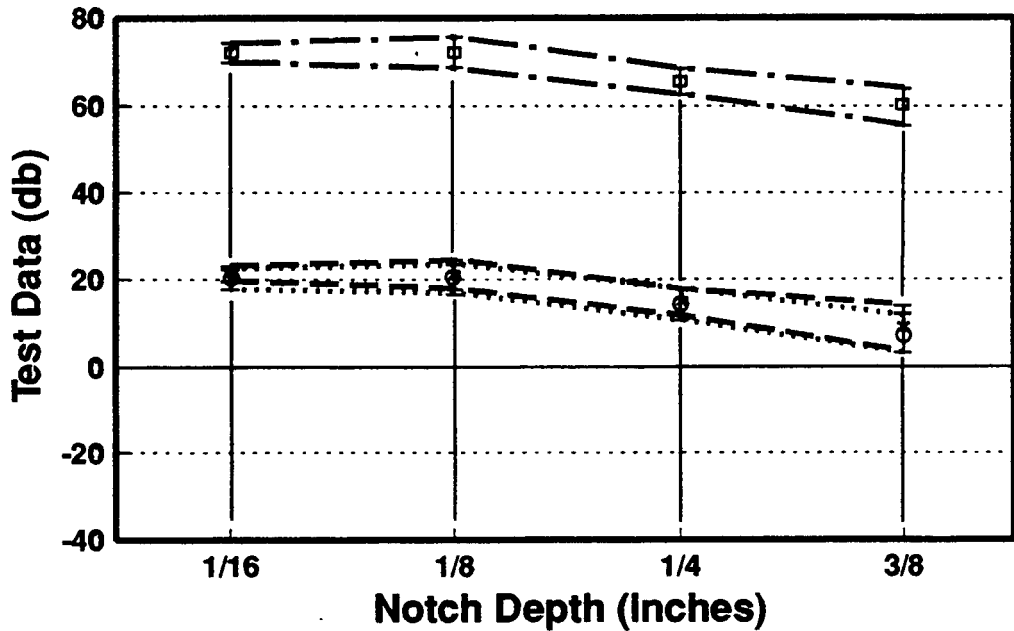
---*--- IDOT Procedure

...○... IDOT Procedure Without Distance Attenuation Correction Factor

Bands Show +/- 1 Std Dev. From Average

Figure 17. Ultrasonic test data for an actual 3-inch diameter pin specimen using a 45 degree angle beam transducer. Figure shows unadjusted data, results from IDOT procedure, and results from IDOT procedure without distance attenuation correction factor.

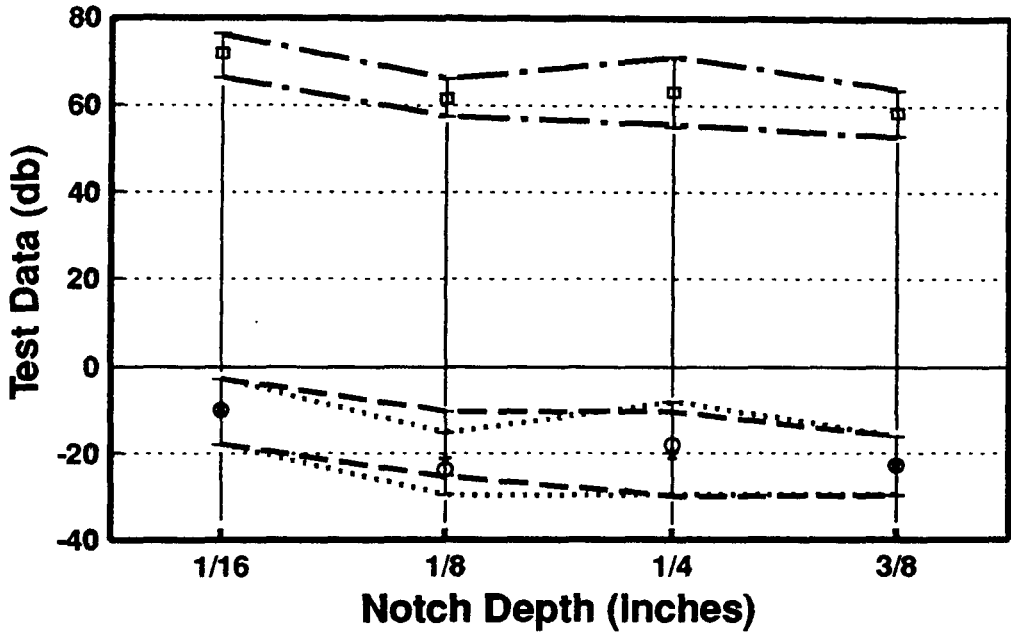
Ultrasonic Data For A572 Plate Specimen Straight Beam Transducer f=3.5MHz



- db Level Required To Put Signal At 50% Screen Height (No Distance or Reference Compensation)
 - *— IDOT Procedure
 - IDOT Procedure Without Distance Attenuation Correction Factor
- Bands Show +/- 1 Std Dev. From Average

Figure 18. Ultrasonic test data for a plate specimen of ASTM A572 steel using a straight beam transducer. Pertinent specimen geometry was the same as that of the tested pin specimen. Figure shows unadjusted data, results from IDOT procedure, and results from IDOT procedure without distance attenuation correction factor.

Ultrasonic Data For A572 Plate Specimen 20 Degree Angle Beam Transducer f=3.5MHz

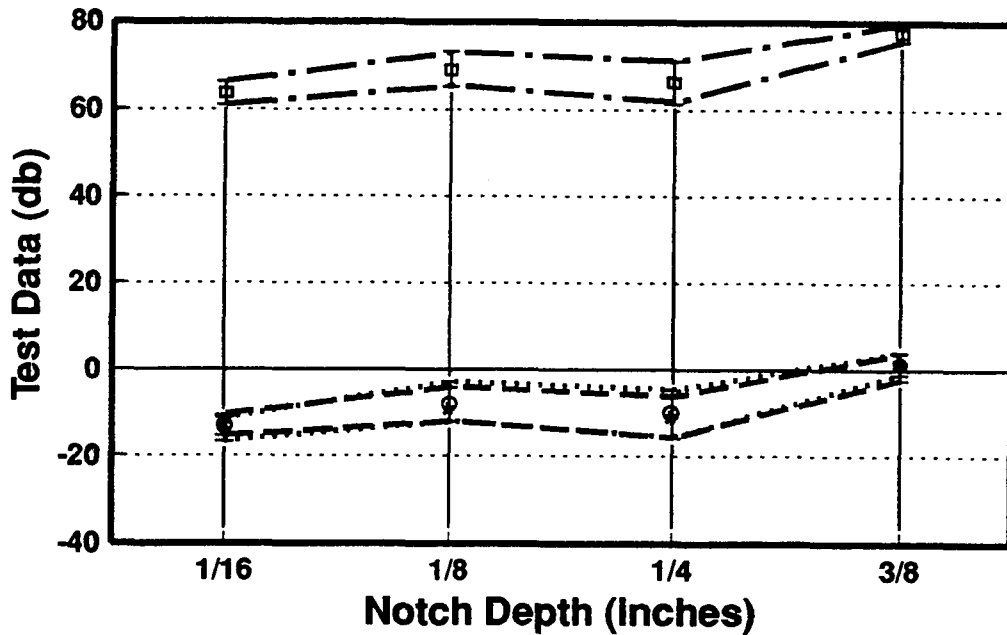


- db Level Required To Put Signal At 50% Screen Height (No Distance or Reference Compensation)
- * IDOT Procedure
- IDOT Procedure Without Distance Attenuation Correction Factor

Note : Bands Show +/- 1 Std Dev. From Average

Figure 19. Ultrasonic test data for a plate specimen of ASTM A572 steel using a 20 degree angle beam transducer. Pertinent specimen geometry was the same as that of the tested pin specimen. Figure shows unadjusted data, results from IDOT procedure, and results from IDOT procedure without distance attenuation correction factor.

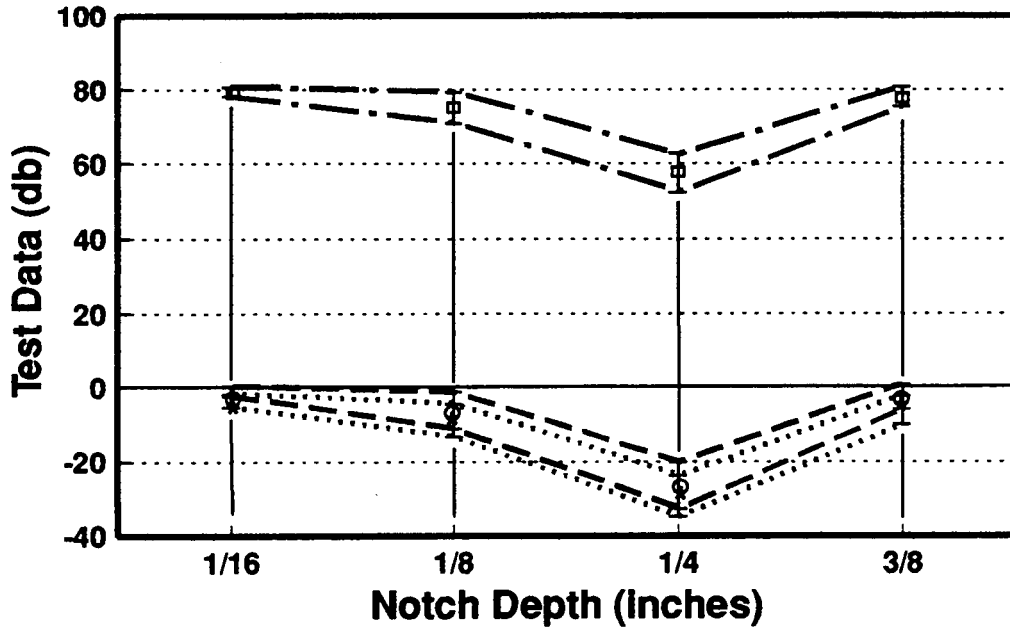
Ultrasonic Data For A572 Plate Specimen 30 Degree Angle Beam Transducer f=3.5MHz



- db Level Required To Put Signal At 50% Screen Height (No Distance or Reference Compensation)
 - *--- IDOT Procedure
 - IDOT Procedure Without Distance Attenuation Correction Factor
- Bands Show +/- 1 Std Dev. From Average

Figure 20. Ultrasonic test data for a plate specimen of ASTM A572 steel using a 30 degree angle beam transducer. Pertinent specimen geometry was the same as that of the tested pin specimen. Figure shows unadjusted data, results from IDOT procedure, and results from IDOT procedure without distance attenuation correction factor.

Ultrasonic Data For A572 Plate Specimen 45 Degree Angle Beam Transducer f=3.5MHz



- db Level Required To Put Signal At 50% Screen Height (No Distance or Reference Compensation)
 - *--- IDOT Procedure
 - IDOT Procedure Without Distance Attenuation Correction Factor
- Bands Show +/- 1 Std Dev. From Average

Figure 21. Ultrasonic test data for a plate specimen of ASTM A572 steel using a 45 degree angle beam transducer. Pertinent specimen geometry was the same as that of the tested pin specimen. Figure shows unadjusted data, results from IDOT procedure, and results from IDOT procedure without distance attenuation correction factor.

6. EXISTING PIN AND LINK EYEBAR DESIGN; RETROFIT REPLACEMENT

This chapter discusses general pin and link eyebar design history, materials of construction, deficiencies with existing pin and link eyebar designs, and introduces new improved designs. In this report, links and link eyebars are considered as interchangeable nomenclature.

General Pin and Link Eyebars Design

The basic pin geometry and link eyebar design prevalent in Illinois bridges is derived from American Institute of Steel Construction design manuals dating back at least 50 years.⁵ The general fit-up of the structural detail consists of a stout pin of carbon steel which fits loosely into a web plate of a beam or girder. The web plate or section may be reinforced by additional boss plates on both sides. The boss plates are typically fillet-welded to the web plate, but may also be riveted or bolted to the web in other designs.

The old design pin connection was purposely designed for looseness of fit to permit free, unrestricted motion and ease of construction assembly. This fit is formally classified as LC11, the widest locational clearance fit for ANSI Standard B4.1-R1979. The pin is initially lubricated before installation, and functions well in the initial part of its life. The pins are inserted into the web, the links subsequently connected, and then the nuts are spun onto a sharply-radiused shoulder and threaded shank. The AISC Standard uses the ANSI 6 threads/inch Unified National Coarse (UNC) series for all pin shank diameters. Another AISC pin design variation for a large diameter pin configuration uses a center hole into which a bar, threaded on both ends, is inserted.

The threaded bar holds down a 0.75-inch thick cap on both ends of the pin. A third AISC design uses cotter pins on both ends of the pin for restraint. Pins are typically lathe-turned or used in the cold-drawn, as-received state. Standard design geometry as shown in Table 8 was extracted directly from the AISC Steel Construction Manual.

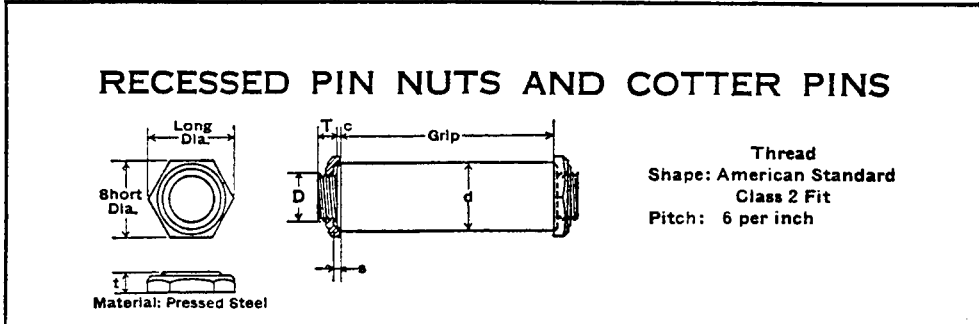
Materials of Construction

Initially, pins and links were machined from plain (unalloyed) low or medium carbon steels, such as ASTM A7 or ASTM A36, or AISI 1045. In a later variation implemented by the Illinois Department of Transportation, pins were carburized using AISI 8620 which was to ostensibly provide a hard wearing surface and a tough pin core. The bearing supporting the pin was a filament wound composite, and impregnated with graphite for self-lubrication. The carburized pin was deeply case hardened to a depth of 0.070-0.100-inch, with a surface hardness of 58 Rc. This high hardness was achieved by quenching in agitated oil and tempering at 300°F. On pins larger than 3.5 inches in diameter, quench cracking was common, with major cracks and spalls emanating from the sharp shoulder. Other serious cracks were also present on other surfaces of the pin. These cracks were noted by inspection before installation and were rejected. Because the pin was not ground to a 32 microinch surface finish or better, observation of micro-cracking was difficult by direct visual methods. Such quench micro-cracks are typically detected by wet fluorescent magnetic particle inspection methods on ground surfaces. Many pins were probably placed in service with existing quench micro-cracks in a deep, carburized case. This case material typically has a carbon content of 0.70 - 0.80%, and has a very low fracture toughness because of its extreme hardness of 58 R_c or above. Such high

TABLE 8

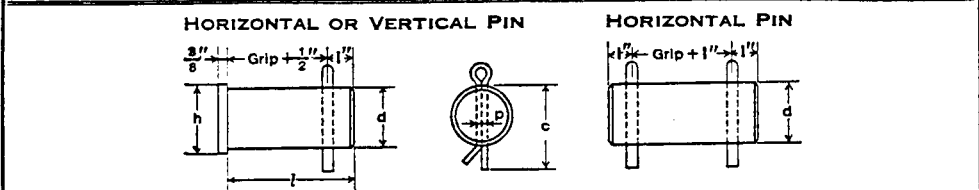
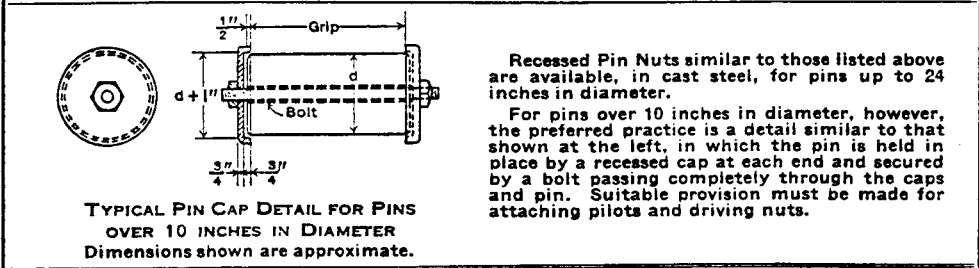
VARIOUS STANDARD PIN GEOMETRIES NOW IN USE.

134



Diameter of Pin <i>d</i>	PIN				Thick-ness <i>t</i>	NUT				Diameter Rough Hole	Weight Pounds	
	Thread			<i>c</i>		Diameter		Recess				
	<i>D</i>	<i>T</i>	<i>c</i>			Short Dia.	Long Dia.	Rough Dia.	<i>s</i>			
2	2 1/4	1 1/2	1	3/8	3/8	3	3 3/8	2 3/8	1/4	1 1/4	1	
	2 1/2	2 3/4	2	1 1/8	3/8	1	3 5/8	4 1/8	3 3/8	1/4	1 3/4	2
3	*3 3/4	3 1/2	2 1/2	1 1/4	1/2	1 1/8	4 3/8	5	3 7/8	3/8	2 1/4	3
	*3 3/4	4	3	1 3/8	1/4	1 1/4	4 7/8	5 5/8	4 3/8	3/8	2 3/4	4
*4 1/4	4 1/2	*4 3/4	3 1/2	1 1/2	1/4	1 3/8	5 3/4	6 5/8	5 1/4	1/2	3 1/4	5
	5	*5 1/4	4	1 5/8	1/4	1 1/2	6 1/4	7 1/4	5 3/4	1/2	3 3/4	6
5 1/2	*5 3/4	6	4 1/2	1 3/4	1/4	1 5/8	7	8 3/8	6 1/2	5/8	4 1/4	8
	*6 1/4	*6 1/2	5	1 7/8	3/8	1 3/4	7 5/8	8 7/8	7	5/8	4 3/4	10
	*6 3/4	7	5 1/2	2	3/8	1 7/8	8 3/8	9 3/8	7 1/2	3/4	5 1/4	12
	*7 1/4	*7 1/2	5 1/2	2	3/8	1 7/8	8 5/8	10	8	3/4	5 1/4	14
*7 3/4	8	*8 1/4	6	2 1/4	3/8	2 1/8	9 3/8	10 7/8	8 3/4	3/4	5 3/4	19
*8 1/2	*8 3/4	9	6	2 1/4	3/8	2 1/8	10 1/4	11 1/8	9 5/8	3/4	5 3/4	24
	*9 1/4	*9 1/2	6	2 3/8	3/8	2 1/4	11 1/4	13	10 5/8	3/4	5 3/4	32
	*9 3/4	10	6	2 3/8	3/8	2 1/4	11 1/4	13	10 5/8	3/4	5 3/4	32

*Special Sizes



l = Length of Pin, in inches.

Pin Dia. <i>d</i>	PINS WITH HEADS		COTTER			Pin Dia. <i>d</i>	PINS WITH HEADS		COTTER		
	Head Dia. <i>h</i>	Weight of One. Lb.	Length <i>c</i>	Dia. <i>p</i>	Weight per 100. Lb.		Head Dia. <i>h</i>	Weight of One. Lb.	Length <i>c</i>	Dia. <i>p</i>	Weight per 100. Lb.
1 1/4	1 1/2	.19 + .35 <i>l</i>	2	1/4	2.64	2 3/4	3 3/8	.82 + 1.68 <i>l</i>	4	3/8	11.4
1 1/2	1 3/4	.26 + .50 <i>l</i>	2 1/2	1/4	3.10	3	3 1/2	1.02 + 2.00 <i>l</i>	5	1/2	28.5
1 3/4	2	.33 + .68 <i>l</i>	2 3/4	1/4	3.50	3 1/4	3 3/4	1.17 + 2.35 <i>l</i>	5	1/2	28.5
2	2 3/8	.47 + .89 <i>l</i>	3	3/8	9.00	3 1/2	4	1.34 + 2.73 <i>l</i>	6	1/2	33.8
2 1/4	2 5/8	.58 + 1.13 <i>l</i>	3 1/4	3/8	9.40	3 3/4	4 1/4	1.51 + 3.13 <i>l</i>	6	1/2	33.8
2 1/2	2 7/8	.70 + 1.39 <i>l</i>	3 3/4	3/8	10.9						

carbon steels are often affected by hydrogen cracking and have minimal shock resistance. The minimum tempering for this hard case should have been 700 - 800°F, but is presently specified at 300°F. The net result for temperatures at 300°F is a brittle case at 58 - 62 Rockwell C hardness. At 700°F, most of the gross residual stresses of quenching are attenuated, and the case is less susceptible to hydrogen embrittlement. Fortunately, the core alloy is AISI 8620, a tough material which can blunt case cracks after they propagate through the brittle case. Pins, whether carbon steel or carburized 8620 pins, receive no other surface treatment to impart some improved corrosion resistance, such as grinding and electroplating, galvanizing, chromating, phosphatizing or electroless nickel. Once the initial lubricant used in construction has weathered away or has been depleted by cyclic motion, the pin receives no other form of corrosion protection.

Deficiencies with Existing Pin & Link Designs

The most serious deficiencies with the existing designs are the loose fit and the resulting gap between the pin, web, and link. This gap permits moisture to accumulate and causes crevice corrosion and accelerated wear. If the grease contains molybdenum disulfide, corrosion of the steel pin may be accelerated due to sulfide attack of the steel if the grease film is dissipated. Since the present pin-plate gap is so large, grease is not held captive. If the grease does not have high viscosity, it can be fluid at temperatures above 120°F. Without a grease film, and with active corrosion taking place, the onset conditions of fretting corrosion can be established.

Many examined pins from Illinois and other states exhibited grooving, which is a direct manifestation of fretting corrosion.

Fretting corrosion is caused by oxides abrading fresh steel from bearing surfaces, which in turn corrode and form additional oxides. These new oxides are then available for further abrasion to perpetuate the cycle. Fretting corrosion is attenuated by decreasing the gap between rotating elements and sealing the gaps with inert lubricants.

Wear and corrosion in pinned connections is further exacerbated by the use of corrosion-susceptible alloys with rough surfaces and loose tolerances, resulting in a poor fit-up. In addition, there are no inherent pin markings, references or strain gages which monitor or indicate motion or movement of pins or link eyebars.

The lubricants that are used in construction are often general purpose lithium-based greases, not extreme pressure lubricants with high viscosity and resistance to atmospheric degradation. A consistent method of retaining lubricants is to keep them captive by preventing their escape by the use of seals and bearing bushings with grease channels.

Many of the previous pin alloys chosen, in addition to having poor corrosion resistance, also have a susceptibility to galling. There is also an absence of toughness specifications for pins, eyebars and web plate materials. Not only are these pin components subject to torsional forces, they undergo shock loads, particularly when the pin-link fit is worn or very loose. For this reason, pins, link eyebars, and pin support and boss plates must have substantial toughness to resist impact loadings. These impact toughnesses should be compatible with their yield strength levels.

Finally, older designs show little regard for removal and replacement. Typically, pins are badly corroded, seized, and must be removed by air arc-gouging. These deficiencies can be remedied by use of

modern pin designs which incorporate automotive, naval, and aircraft design practices.

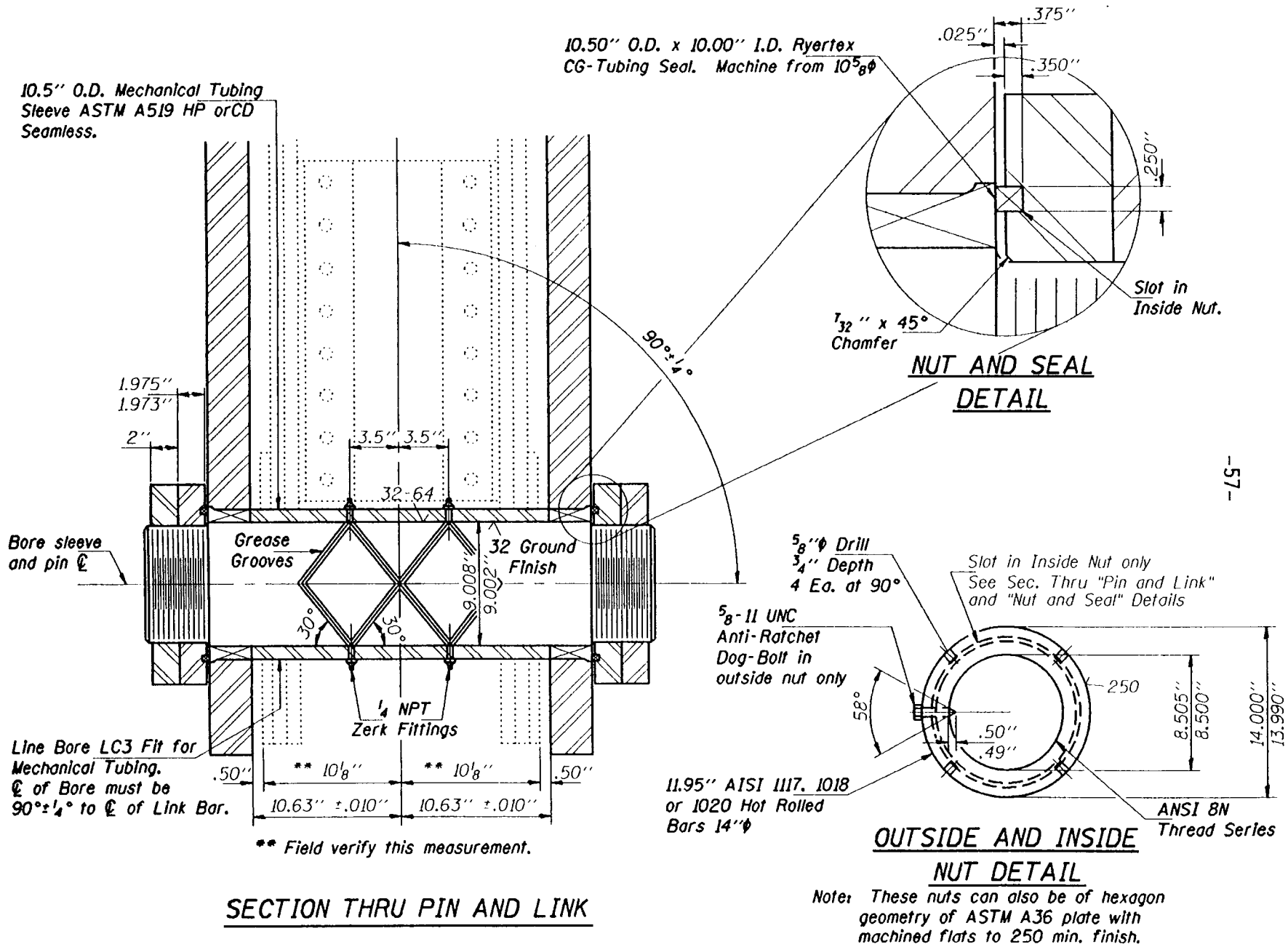
New Pin and Link Eyebar Designs

In the modernized designs, many of the existing deficiencies are eliminated. These improvements include (a) better tolerances on fits and finishes, (b) increased degrees of freedom of rotation, and (c) provisions for periodic lubrication. The bearing materials are stainless steels or bearing bronzes. The pin materials are either quenched and tempered steel alloys that rely on lubricant presence for corrosion inhibition, or are stainless steel or aluminum bronze.

In Figure 22, a typical new 9-inch diameter pin detail is shown. The pin has a minimum of two degrees of rotational freedom for redundancy of motion. The link eyebar rotates about the pin, and the pin rotates in a machined steel sleeve bearing. Additional degrees of freedom can be obtained by eliminating the shrinkfits. The minimum clearance is .010-inch, which is within the tolerances of an ANSI RC 8 fit. An ANSI RC 8 fit is a loose running clearance, which accommodates the distortion of shrinkage and inaccuracies of line boring. This fit provides sufficient clearance for the pin after the sleeve bearing is inserted into the web. The sleeve is grooved in the central portion away from the line of bearing action passing through the web. The zerk fittings on either side are available to purge grease if necessary.

The sleeve is not fillet-welded to the web to prevent any kind of weld toe cracking which could propagate into the structural member. Moreover, the line boring of the web elements insures that a true center and circularity of the hole is achieved, which could never be guaranteed

Figure 22. A typical new 9-inch diameter pin connection detail.



by flame or plasma cutting. The pin passes through the link eyebar bearing and is secured by two nuts. The first nut is specially chamfered so that when it is tightened, it provides a clearance of approximately .025" for a grease seal made of Ryertex CG, a synthetic machinable composite that is impregnated with graphite. The outer nut is also circular to limit torque. A special wrench that applies 450 ft.-lbs. nominal torque is provided, as shown in Figure 23. The wrench is designed so that if too much torque is applied, the AISI 41L50 cold finished bar insert will shear off. These pin nuts can also be fabricated from plate steels into a hexagonal form, and torque can also be limited by wrench handle length. These nuts interface with the bronze bearing insert in the link eyebar, forming a corrosion-resisting seal to exclude moisture. This nut and seal arrangement is shown in Figure 24. An additional safety precaution is built into the nut by the use of anti-ratchet dog bolts.

The pin itself, as detailed in Figure 25, is a ground and polished round bar made of AISI 9310, a low carbon, 3% nickel and 1% chromium alloy steel with high toughness, particularly in the normalized or quenched and tempered state. When specified as aircraft quality, the pin is inspected for surface flaws. The bearing surfaces are ground to a 16 micro-inch finish, minimizing both seizure and corrosion. The radiused portion of the pin has only a 0.25-inch radius. Previous pin designs showed a much sharper step which reduces the scanning ability of an ultrasonic transducer to search for cracking. The reduced gentle radius now permits full straight beam scanning for internal cracks or flaws.

The link eyebar, as described in Figure 26a, is probably the most vulnerable detail to rupture. Its highest area of stress concentration

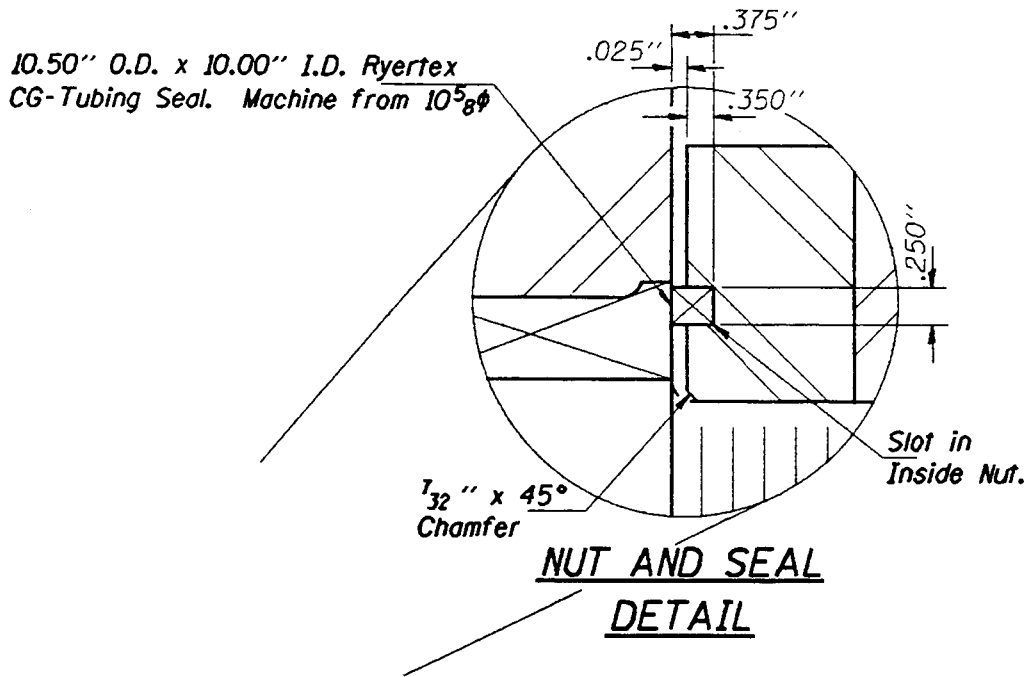
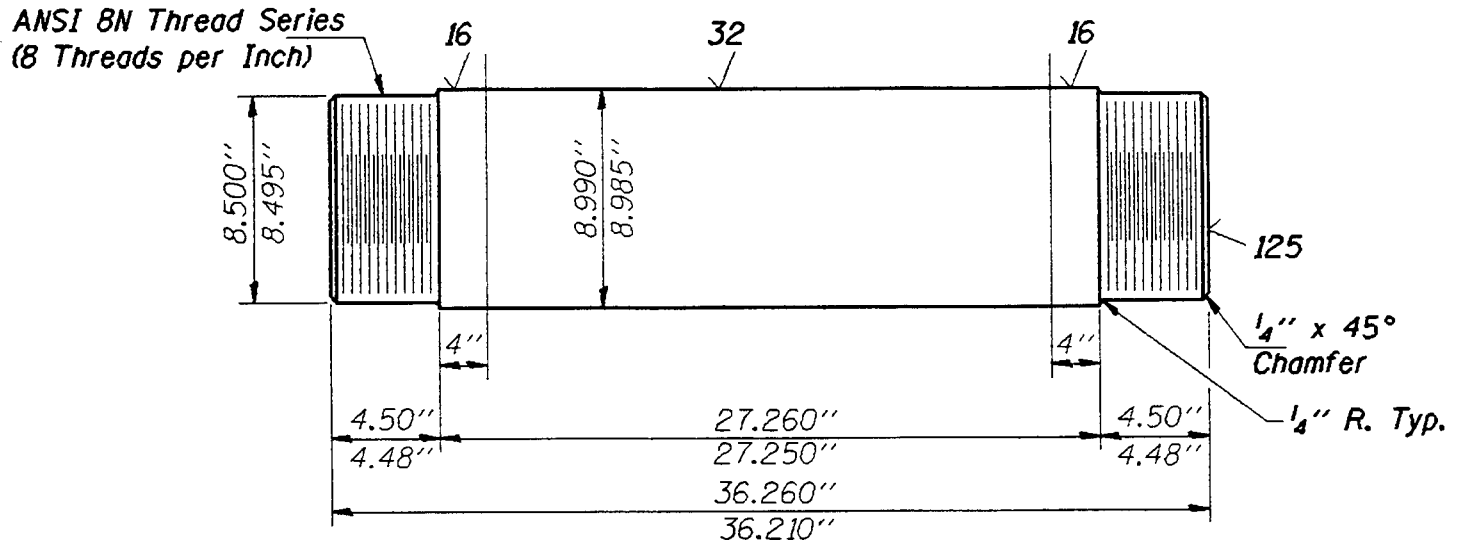


Figure 24. Nut and seal detail for moisture exclusion.



PIN DETAIL

Pins shall be AISI 9310 normalized and tempered, aircraft or bearing quality 250 BHN min., 80 ksi yield strength min., 17% elongation min. or AISI 4620 normalized and tempered, aircraft quality, 183 BHN min., 63 ksi yield strength min., 22% elongation min. Toughness Requirement: 45 Ft.-Lbs. at 0° F. CVN.

Figure 25. Nine-inch diameter pin detail also showing material properties and surface finish requirements.

is at the 90° position, where strain gages are mounted to monitor any plate stress changes. The peak stresses are shown in a finite element model of the eyebar in Figure 26b. Gages are located a distance from the nuts to prevent strain gage wire seizure. The lubrication port was placed at the minimum stress position (at 0°) to decrease the likelihood of crack formation in the grease hole. The link eyebar is made of AISI 4130 aircraft quality normalized plate. This material has good hardenability and toughness, with significantly improved machinability, compared to similar low carbon alloy steels (55% to 70%). ASTM A514 plate is also another alternative alloy. The link is machined flat by surface milling. This permits excellent alignment and true perpendicularity on bearing bores and bushings. In addition, the surface finish is improved to 64 micro-inches in the areas of maximum tensile stress. Also, the internal bore surfaces are inspected by wet fluorescent magnetic particle methods for any internal flaws exposed by the boring of the plate. Lastly, the link eyeplate and the pin have a toughness requirement of 45 ft.-lbs. at 0°F by the Charpy V-notch impact test, a level commensurate with its yield strength as per the unified Fracture Criteria Impact Test Requirements of Table S1.3 of ASTM A709, Structural Steel for Bridges.

The advantage of this design compared to existing pin designs is that it has close tolerances, will exclude moisture, and will have reduced friction for long periods of time. A variety of alloys can be used for link eyebars, pins, and bearings that are both strong, tough, and corrosion resistant. These alloys are summarized in Table 9.

The lubricants selected are extreme pressure greases that have also shown good performance in adverse environments. Lubricant properties are derived from established commercial technical literature. The lubricants are summarized in Table 10.

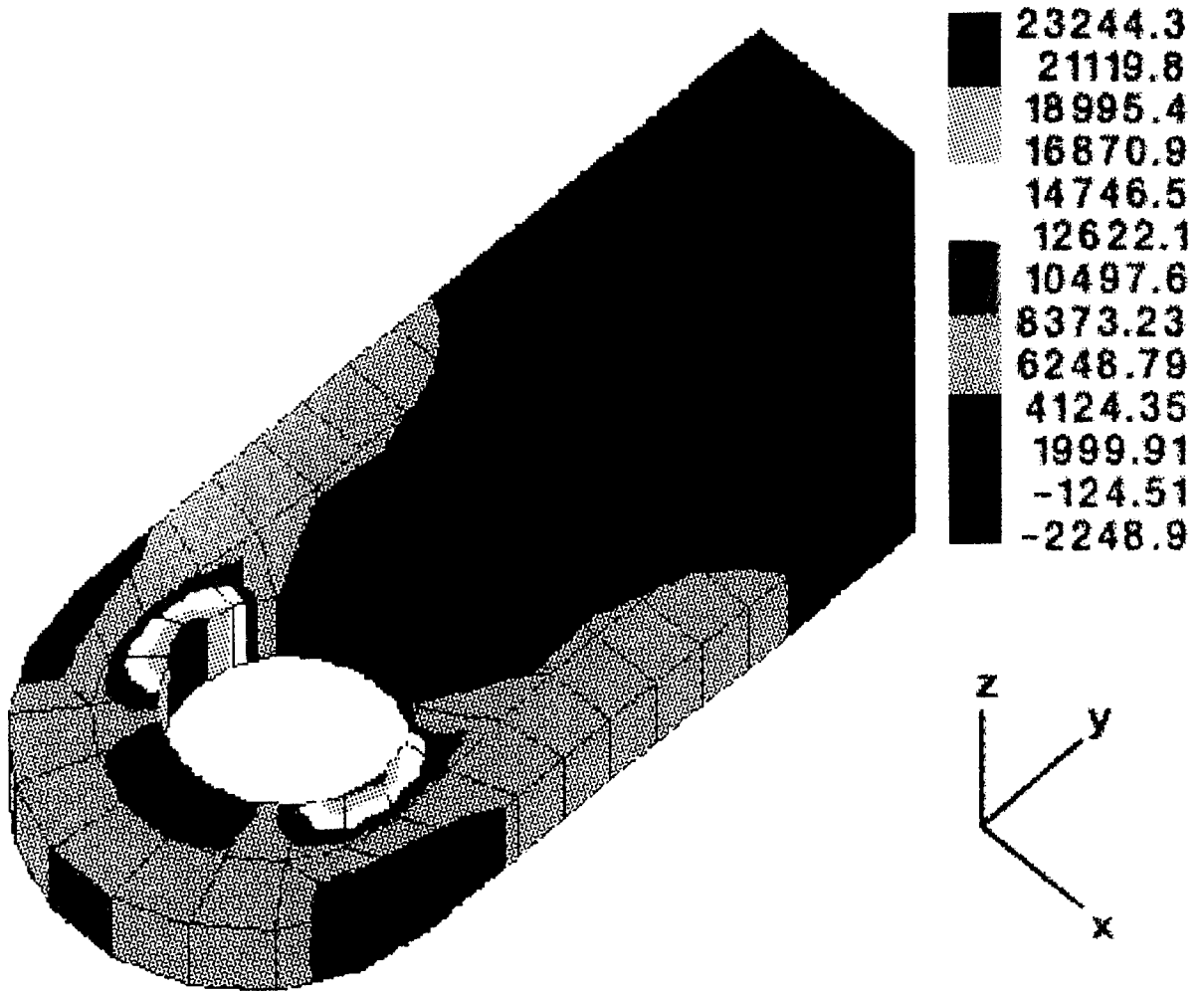


Figure 26b. Finite element model of the link eyebar. Stresses are for maximum loadings for the Peru Bridge. Note that eyelet peak stresses are about 3X nominal stress. Stress values in the legend are in psi.

TABLE 9

PIN, LINK, AND BEARING ALLOYS

<u>Component</u>	<u>Alloy</u>	<u>Characteristics</u>
Pin	Nitronic 60	corrosion resistant; galling resistant; 60 ksi yield strength; good toughness; high cost/lb
Pin	AISI 8620, quenched & tempered & stress relieved	tough, low cost; about 85 ksi yield; about 2X corrosion resistance of A36
Pin	Ferralium Alloy 255 duplex stainless; or Sandvik SAF 2205	high corrosion resistance, tough, weldable; higher cost grades; may be susceptible to galling
Link	AISI 4130 ASTM A514	tough, strong (to 100 ksi); 2x better corrosion resistance than A36
Link	AISI 9310 or AISI 8620	very tough steel; about 2x corrosion resistance of A 36
Bearings	ASTM B16 (UNS 36000); ASTM B121, Alloy C35300	leaded for free machining; good bearing properties, but lower yield; corrosion resistant
Bearings	Nitronic 60	corrosion resistant; gall resistant
Bearings & Pins	Ampco 954	corrosion resistant; strong for brass alloy (40 ksi yield); bearing properties not as good as leaded brasses; costly as pins
Pins, Plates & Reinforcing Bosses	ASTM A808; ASTM A808; ASTM A514	strong, tough alloys with atmospheric corrosion resistance 2X ASTM A36.

TABLE 10

PIN AND LINK LUBRICANTS*

<u>Manufacturer</u>	<u>Product Name</u>	<u>General Characteristics</u>
Jet-Lube Houston, TX	202 Moly-Lith	Low friction, high load with extreme resistance to heat, water, weathering and oxidation.
	ALCO-EP 73 Plus	Molybdenum disulfide & graphite in an aluminum complex base; suited for subseawater applications.
Keystone Div., Pennwalt Corp. King of Prussia, PA	Zeniplex-2	Carries extreme pressures with high water and moisture resistance.
	81-EP 2	Lithium base grease extreme pressure; resistance to moisture and mild acids & alkalis; contains anti-rust inhibitors.
Mobil Corp. New York, NY	Mobilux EP 2	Lithium base extreme pressure grease with oxidation and rust inhibitors.
Tech-Lube Islip, NY	T-800-S	Waterproof grease; resistant to acids, alkalis; compatible with brass and bronze.

*Note: Lubricants are listed only in alphabetical order; characteristics are based on descriptions for manufacturer's technical literature only and have not been confirmed by independent government testing.

The pins themselves must be ground to at least a 32 micro-inch finish. The strength of the pin should be sufficient to satisfy primarily the shear forces, although torsional forces from seizure can be significant. At maximum anticipated loadings, the shear stress should not exceed 35% of the yield strength. The impact and fracture toughness of the pin and eyebar is a function of its yield strength and the surrounding temperature.

Pins, bearings, and links can also be marked for motion sensing; and strain gages can be welded and sealed on eyebars to detect any excessive strains due to lockup or outright seizure.

For pins or link eyebars that are fracture critical, the impact toughness requirements, preferably taken transverse to the bar or plate's rolling direction, should conform to the requirements of the supplemental tables of ASTM A709. Similar reduced values for non-fracture critical pins and link eyebars are also published in this standard, which is summarized in Table 11 for Zone 2 (Illinois).

Actual pins, link eyebars and nuts fabricated and machined in accordance with the new designs are shown in the following set of figures. These components are being used in the Peru Bride Rehabilitation Project. In Figure 27, the ground and threaded AISI 9310 pins are readied on pallets for delivery. A closeup of a single pin is shown in Figure 28. The large diameter circular nuts that spin onto the ends of the pins are shown in Figure 29. Note the internal groove where the Ryertex graphite seal fits. Figure 30 shows how the special chamfer on the nut when it runs into the pin radius forms a gap for the Ryertex seal. This prevents overtightening and lockup of the nut against the link eyebar. Figure 31 shows two milled and bored link eyebars prior to acceptance of the bearing inserts into the eyelets. Figure 32 is a stack of 4 bearing inserts which are shrunk fit into the link eyebar. Note the internal grease groove.

TABLE 11

IMPACT TOUGHNESS REQUIREMENTS FOR PIN AND LINK MATERIALS
FOR TEMPERATURE ZONE 2*

<u>Yield Strength Range, ksi</u>	<u>Thickness</u>	<u>Average Energy, ft.-lbs.</u>	
		<u>Non-fracture Critical</u>	<u>Fracture Critical</u>
36 - 49	up to 4"	15 @ 40°F	25 @ 40°F
50 - 69	to 2" (welded/bolted)	15 @ 40°F	25 @ 40°F
	to 4" (bolted)	15 @ 40°F	25 @ 40°F
	to 4" (welded)	20 @ 40°F	30 @ 40°F
70 - 99	to 2 1/2" (welded/bolted)	20 @ 20°F	30 @ 20°F
	to 4" (bolted)	20 @ 20°F	30 @ 20°F
	to 4" (welded)	25 @ 20°F	35 @ 20°F
100 - 130	to 2 1/2" (welded/bolted)	25 @ 0°F	35 @ 0°F
	to 4" (bolted)	25 @ 0°F	35 @ 0°F
	to 4" (welded)	35 @ 0°F	45 @ 0°F

*Based on Tables S1.2 and S1.3 of ASTM A709, Structural Steel for Bridges.

Safety Criteria for Pins and Links

A pin and link eyebar are subjected to a variety of forces throughout their lifetimes. The principal pin forces are (1) bending stresses induced by the offset distance between the web's line of action and the link's line of action; (2) the shear forces on the pin itself; (3) the torsional forces which develop on the pin from friction or permanent seizure at the pin-link interface. The principal link eyebar forces are (1) tensile and compressive stresses from loading and (2) torsional forces resulting from friction or actual seizure with the pin due to poor lubricity as the link moves due to thermal expansion of the bridge. See Figure 33. These shear and tensile stresses have both a steady stress component derived from dead load and an alternating stress component originating from live loads. The torsional stress is also alternating, since it is derived from rotation induced by thermal expansion.



Figure 27. Machined and finely ground pins for Peru Bridge.

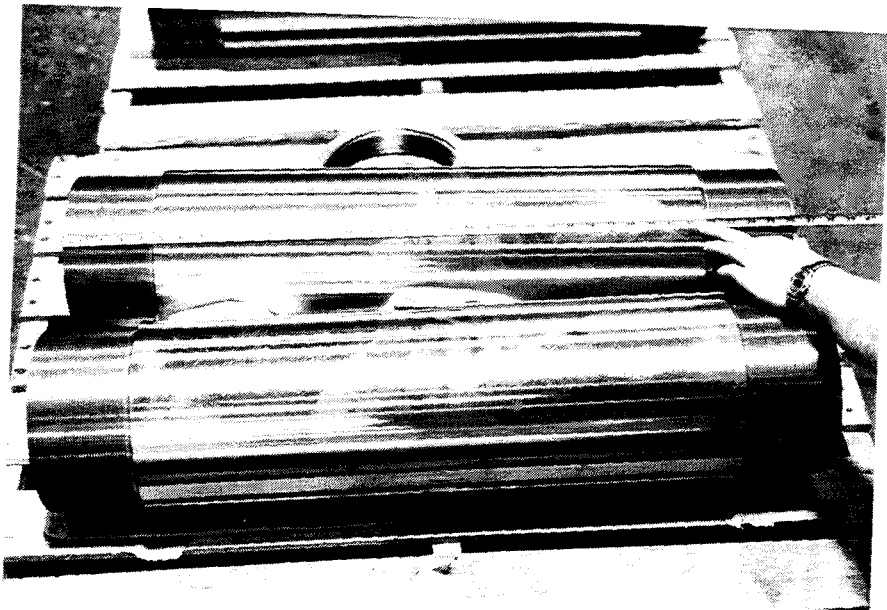


Figure 28. Closeup of pin and general size.



Figure 29. Circular nuts for pins. All grooves and holes for dog bolts were not yet machined out.



Figure 30. Special chamfer which permits a space for a grease seal situated between the nut and link eyebar.

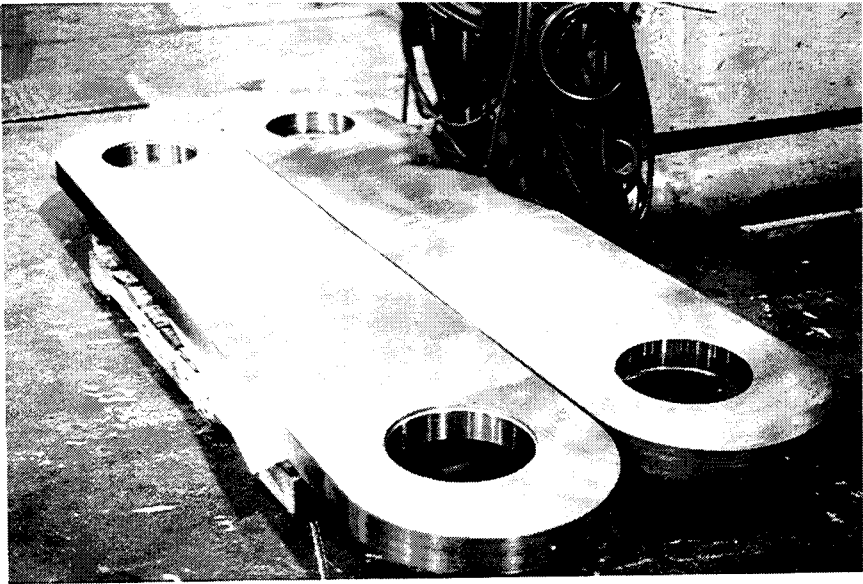


Figure 31. Machined link eyebars, milled to be completely flat and with radii with smooth finishes. Bearings have not yet been inserted in this picture.



Figure 32. A stack of four bronze bearing inserts, showing internal grease groove.

Link eyebar tensile stresses are at their maximum at the 90° & 270° positions. The equation predicting such maximum stresses is⁶:

$$S_{\max} = \frac{W \Psi}{\lambda r B}$$

where: W = Weight on link, lbs.
Ψ = Stress factor, a function of the clearance ratio, $n = e/r$ (See Fig. 34).
e = clearance between pin and link, inches
r = radius of pin, inches
λ = $12/r$ or ratio of link radius outside R to inside radius r
B = thickness of link, inches

A consequence of loose clearance between pin and link eyebar is a progressively increasing stress level in the link eyebar.

Shear and bending forces are determined conventionally. Torsional forces on the pin are determined by making an estimate of the coefficient of friction between the link eyebar and pin. Torque is applied when frictional forces on the periphery of the pin increase as the surface is degraded by roughness, corrosion and the seizure of surface asperities from pin to link. The peripheral surface forces are determined by the relationship $F = \mu N$ where N is the normal force and μ is the coefficient of friction. These coefficients vary widely from material to material, and by lubricant and surface conditions. The coefficients of static friction for various material combinations used in pins is shown in Table 12.

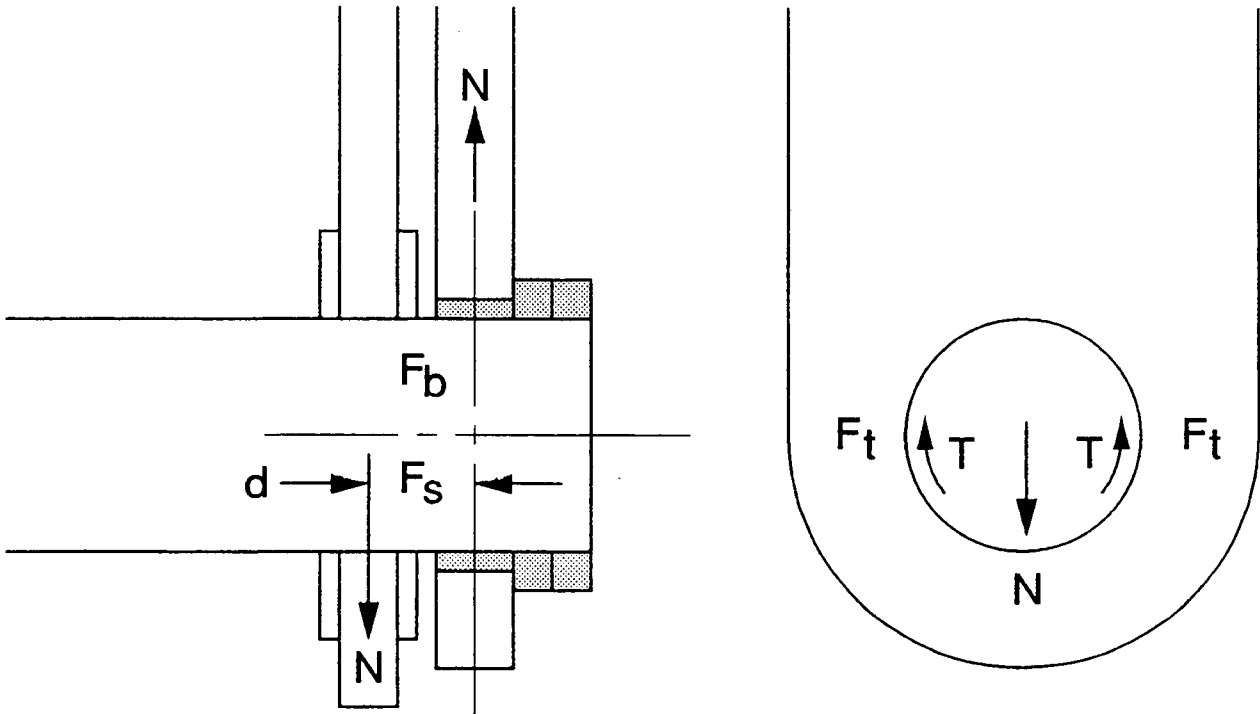


Figure 33. Principal forces and stresses on pins and link eyebars. N is the normal force exerted on the bearing; F_b is the bending stress on the pin; F_s is the shear stress on the pin; F_t is the torsional force on the link; T is the torsional stress on the pin.

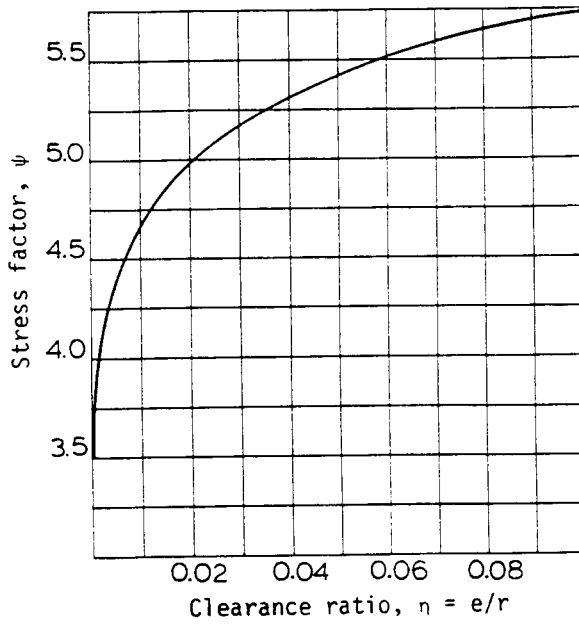


Figure 34. Stress factor for typical eyebar design (Ref. 6, page 376).

TABLE 12

TYPICAL COEFFICIENTS OF STATIC FRICTION (μ)

<u>Material Combination</u>	<u>Dry</u>	<u>Lubricated</u>
hardened steel on hardened steel	0.78	0.11 - 0.23
mild steel on mild steel	.74 - 1.2	0.09
hardened steel on graphite	0.21	0.09
hardened steel on babbitt	0.42	0.08 - .17
mild steel on bronze	.45 - .51	.11 - .13
aluminum on aluminum	1.9	---

Data sources: Handbook of Chemistry and Physics; Mark's Mechanical Engineers Handbook.

The forces that impinge on a pin are multiple. The safety of a pin is best determined by its combined distortion energy. A reasonably conservative relationship for safety factor for shafting ⁷ is as follows:

$$n = \frac{1}{[(\sigma_0/\sigma_u + K_{tf} \sigma_v/\sigma_e)^2 + 3(\sigma_0/1.33\sigma_y + K_{tf} \sigma_v/\sigma_e)^2]^{1/2}}$$

where: σ_0 = steady bending stress, due to dead load

σ_u = ultimate tensile strength

σ_v = alternating bending stress, due to live loads

σ_e = fatigue strength at 10^7 cycles; for pins approximately $\sigma_u \times [.3]$ subject to minor corrosion

σ_0 = combined steady shear and torsional stresses

σ_v = alternating shear or torsional stress, due to live loads

σ_y = yield strength

K_{tf} = clamping factor for bearings; is 1.0 for shafts with no notches

A more simplified safety factor equation can be used for link eyebars. The Gerber parabola fatigue failure equation is widely used in this case.

$$n = \frac{1}{(\sigma_m/\sigma_u)^2 + (\sigma_a/\sigma_e)}$$

- where: σ_m = mean stress, where $(\sigma_D + \sigma_{LL} + \sigma_F) / 2 = \sigma_m$
 σ_D = peak tensile stress from dead load at 90° position
 σ_{LL} = peak tensile stress from live load at 90° position
 σ_F = tension from friction due to lack of lubrication or corrosion or both in eyelet.
 σ_a = alternating stress, where $\sigma_{LL}/2 + \sigma_F/2 = \sigma_a$
 σ_u = ultimate tensile strength
 σ_e = fatigue strength at 10^7 cycles, where $\sigma_u \times [.3]$.

As a rough approximation, 10% of the live load stress may be added to compensate for frictional forces in a lubricated pin. For pins and links these values should not fall below $n = 1.50$ because many of the coefficients of friction are estimates and fatigue strengths of very high strength materials often level off at $\sigma_u = 150$ ksi or greater. For pins suspected of higher frictional forces, the link eyebars should be either instrumented with strain gages or monitored with photoelastic coatings to note peak stress levels.

7. SUMMARY

Pin connections on bridges in Illinois are a potentially serious problem. Many failures of both pins and link eyebars have been reported throughout the country as shown in NCHRP 333. These connections were designed to move freely in response to traffic and thermal movements, but years of corrosion and wear usually result in at least a partially fixed condition. This fixity introduces unintended bending stresses in the hangers or link eyebars and shear stresses in the pins.

Several methods of detecting relative movement or rotation were developed and field tested in order to study actual pin connection behavior. Strain gages and electronic rotation sensors were found to be most suitable for gathering quantitative data. Strain gage installations were better suited for further stress analysis.

Finite element models of three actual structures were employed to estimate the maximum effect of fixity on pins, hangers, and link eyebars due to live load and thermal movement. A thermal differential of fifty degrees Fahrenheit was used in all models. Analysis of this data reveals that complete fixity can create a highly dangerous condition for both pins and hangers or link eyebars in a given connection. Partial fixity also induces high stresses which may cause yielding in a component and/or accelerate fatigue damage, depending on the degree of fixity. Analysis of strain gage data collected from installations on the I-270 and I-474 bridges showed that pins do experience shear stresses due to thermal changes. These shear stresses ranged from approximately 0.4 ksi to 11 ksi in magnitude.

Previous researchers showed that the most practical way to inspect pins for defects was by ultrasonic methods. An inspection and calibration procedure was developed and implemented. Two pilot contracts were let for

pin inspections during the summers of 1989 and 1990. Results of these inspections revealed relatively few defects of appreciable size and no complete failures.

The inspection procedure provides a calibration block. It calibrates both longitudinal and angle beam transducers to a 1/16-inch hole to provide a degree of repeatability. Angle beam and straight beam techniques were used because of the many pin sizes and configurations in use in Illinois. The pin inspection procedure is presently undergoing further refinement.

Existing pin designs and materials used in Illinois bridges were reviewed. The basic pin and link eyebar geometry and design date back at least 50 years. Several deficiencies of the current designs and materials were noted. The most serious deficiencies with the existing designs are the loose fit and the resulting gap between the pin, web, and link eyebar. This condition allows any lubricants present to dissipate, and the accumulation of moisture, causing crevice corrosion. The large gap also allows fretting corrosion to occur. The lubricants used, if any, are often general purpose greases which may not have sufficient resistance to atmospheric degradation. The alloys presently specified are corrosion-susceptible and have rough surfaces and loose tolerances. These conditions result in poor fit-up. Many of the alloys used are also susceptible to galling. There are no toughness specifications for pins, links, or web plates. The designs show little regard for pin and link eyebar removal and replacement.

A modernized design was presented in which many of the existing deficiencies are eliminated. The improvements include better tolerances on fits and finishes, increased degrees of freedom of rotation,

provisions for periodic lubrication, higher strength, more corrosion-resistant alloys, and the use of extreme pressure lubricants. Toughness requirements based on alloy yield strength were also presented.

8. CONCLUSIONS

Based on the work done in this report, the following conclusions are made:

- 1) The effects of pin fixity can be quantitatively measured by a strain gage circuit and strain gages mounted on hangers or link eyebars.
- 2) In cantilever truss bridges, completely fixed pins are subjected to varying stress levels, depending on structure length, pin material properties, and pin diameter.
- 3) Cantilever girder bridges may experience conditions which could result in yielding and permanent deformation due to the combination of complete fixity and live load.
- 4) Hangers or link eyebars, in addition to pins, are at risk due to fixity due to cyclic fatigue stressing in the yielded stage.
- 5) Partial fixity effects could result in fatigue damage of hangers or link eyebars.
- 6) The pin inspection procedure requires more work for correlation between defect size and test data.
- 7) Based on the results of the pin inspection contracts, there are relatively few pins in Illinois with serious defects, and no complete fractures.
- 8) Existing pin connection designs have deficiencies which allow crevice corrosion, fretting corrosion, and fixity to occur.
- 9) New pin connection designs, using standard automotive, naval, and aircraft designs for bearings, provide more degrees of freedom of rotation, access for lubrication, and alloys with high toughness, galling resistance, and corrosion resistance.

- 10) The toughness of the entire assembly, including pins, link eyebars, pin plates, boss plates or sleeves, should have sufficient toughness to resist impact. Impact toughness levels should be compatible with the alloys yield strength and the lowest temperature that the bridge will encounter, preferably meeting the standard of ASTM A709, Tables S1.2 and S1.3.

REFERENCES

- ¹ Carroll, F., Martin, F., McDonald, S., "Non-destructive Bridge Pin Testing." Public Works, Volume 120, Number 1, January 1989.
- ² Ross, C.T.F., "Applied Stress Analysis." Halsted Press, New York City, New York, 1987, p. 309.
- ³ Shigley, J., Mitchell, L., "Mechanical Engineering Design." 4th edition, McGraw-Hill Book Company, New York City, New York, 1983, p. 842.
- ⁴ Kulicki, J., Prucz, Z., Sorgenfrei, D., Mertz, D., Young, W., "Guidelines for Evaluating Corrosion Effects in Existing Steel Bridges." NCHRP Report Number 333, Transportation Research Board, Washington, D. C., 1990, pp 92-94.
- ⁵ Steel Construction Manual, 2nd Edition, AISC, New York City, New York, 1934, pp. 114-115.
- ⁶ Blake, A., "Practical Stress Analysis in Engineering Design." 2nd edition, Marcel Dekker, Inc., New York City, New York, 1990, p. 376.
- ⁷ Marks Standard Handbook for Mechanical Engineers, 8th Edition, McGraw-Hill, New York, 1978, pp 8-49
- ⁸ Collins, J., Failure of Materials in Mechanical Design, John Wiley, New York, 1981, pp 218.

APPENDIX A

ULTRASONIC TEST PROCEDURE FOR PINS

1. Equipment Required for Ultrasonic Testing:
 - a. Krautkramer-Branson USK7 flaw detector or equivalent.
 - b. 1/2" diameter, 3.5 MHz transducer for straight beam application, Gamma-HP series or equivalent.
 - c. Miniature Shear Wave Transducers:
20 - 30 - 45 and a 1/2" diameter, Angle beam, with wedges for 3.5 MHz transducer. The quick change type is recommended, with interchangeable wedges.
 - d. The couplant shall be a heavy bodied, pourable, water soluble, non-corrosive, nontoxic grade suitable for vertical surfaces. KB-Aerotech's Exosen #30 or equal is recommended.
 - e. A specially made distance and sensitivity calibration block for pins "DSC-P" to be furnished by the Department.
 - f. Ultrasonic Inspection Report Forms furnished by the Department.
2. Calibration - Straight Beam Transducer

The calibration of the straight beam transducer is dependent upon the depth of shoulder to root (dimension "S", Figure A2) of the threaded portion of the pin. If the "S" dimension of the shoulder is greater than 3/8" (0.375), the calibration shall be referenced to the 0.06" diameter hole located 5" from the end as shown in Figure A1, position A. The 3" sound path is used if the depth of the shoulder is equal to or less than 3/8" (0.375) as shown in Figure A1, position B.

In either case, the gain of the instrument should be adjusted so that the return signal is viewed as 50% of the vertical scale or mid-height of screen. The adjustment shall be made with the transducer placed flush with the end of the calibration block. The "Reference Level" shall be taken from the gain (attenuation) indicators of the instrument with the signal at 50% screen height.

For pins equal to or less than 10" in length, the horizontal scale should be set for the full scale width indicated on the screen. The horizontal scale will have to be proportioned for pins exceeding 10" in length.

3. Calibration - Angle Beam Transducer

The calibration of the shear wave transducers for "Reference Level" is determined directly from the instrument's gain indicator. After the transducer angle has been chosen based on pin geometry for the pin area in question the test block sound path closest to the anticipated sound path distance is used to establish the "Reference Level". The gain is then adjusted until the maximum return signal is viewed as 50% of the vertical scale.

The sound path distance used for calibration shall be recorded on the UT report in the column below the transducer angle.

Example: A 30° Wedge angle was determined to give the necessary coverage in the area subject to the most corrosive wear, and a sound path of approximately 3 1/2" was chosen to scan the region. Calibration is accomplished by placing the transducer on the side of the block at the point intersecting the 3 7/16" sound path line. The gain of the instrument is adjusted until the maximum return signal of the deficiency is viewed as 50% of the vertical scale. The "Reference Level" is read directly from the instrument and recorded on the UT reports. A 3 7/16" is recorded below the 30 column. (Figure A1, position C)

4. Ultrasonic Test Procedure: General

The ends of pins to be tested shall be free of accumulated paint, rust burrs, and any roughness than would prevent the transducer from making full contact and restricting movement across the surface. During scanning, the gain of the instrument is to be set approximately 20 db above the Reference Level. Each pin end shall be scanned with both a straight beam and at least one angle beam transducer. The scanning level should be recorded under "Remarks".

Apply an approved couplant to the surface of the end of pin being tested. Position the transducer on the end of the pin and slowly move it over the entire area of the pin with an even amount of pressure to keep the couplant under the transducer while testing is in progress.

An "Attenuation Factor" of 2 dB per inch of sound travel less than or greater than the calibration length shall also be recorded on the form. The attenuation factor shall be recorded as a minus value if the sound path is greater than the sound path used for calibration or when the path is less than the sound path used for calibration. The "Indication Rating" shall be taken as the Indication Level minus the difference between the Reference Level and the Attenuation Factor.

Example: The gain of the instrument is adjusted to 70 dB so that the maximum return signal of a defect, is viewed at mid-height of the screen. The Reference Level, determined on the test block, is 56 dB after applying a straight beam adjustment factor. The sound path is one inch longer than the calibration sound path setting the Attenuation Factor equal to 2 dB. The "Indication Rating" is $70 \text{ dB} - (56 \text{ dB} - 2 \text{ dB}) = 16 \text{ dB}$

5. Straight Beam Testing

The CRT screen reading for a good pin will show an initial pulse signal and reflections from the threaded reduction shoulder and the end of the pin. The reading for a pin with a defect at the hanger plates will show a signal at the location of the defect. If the defect extends below the shoulder, the reflective signals from the shoulder will be lost due to the return signal from the flaw.

A pin that has an indication between the initial signal and the signal from the far shoulder is evaluated by adjusting the gain either up or down until that signal is at mid-height on the CRT screen. The amount of gain that it takes to bring the indication to mid-height is recorded on the report under "Indication Level". The location of the signal from the horizontal base line on the CRT screen will correspond to the distance of the indication from the end of the pin and is recorded on the UT report as "Location from A" or "Location from B".

6. Shear Wave Testing (Angle Beam Testing)

The transducer is moved with even pressure along a diametral line starting at the 12:00 position, See Figure A2, and rotating clockwise around the end of the pin until the entire surface of the pin is covered. The transducer should not be lifted off the face of the pin end. The scanning motion is as follows: 12:00 to 6:00, 7:00 to 1:00, 2:00 to 8:00, etc. It is essential that a generous amount of couplant be maintained between the surface of the pin and the transducer at all times, especially if the ends of the pins are pitted from rust or original fabrication. The sound path to the defect is recorded under "Sound Path". Special measures are necessary to scan pins with cotter pin holes, centering holes from original machining, extremely long threads, no turned-down shoulders, or end caps with capture bolts. Procedures for these situations shall be coordinated with the Engineer.

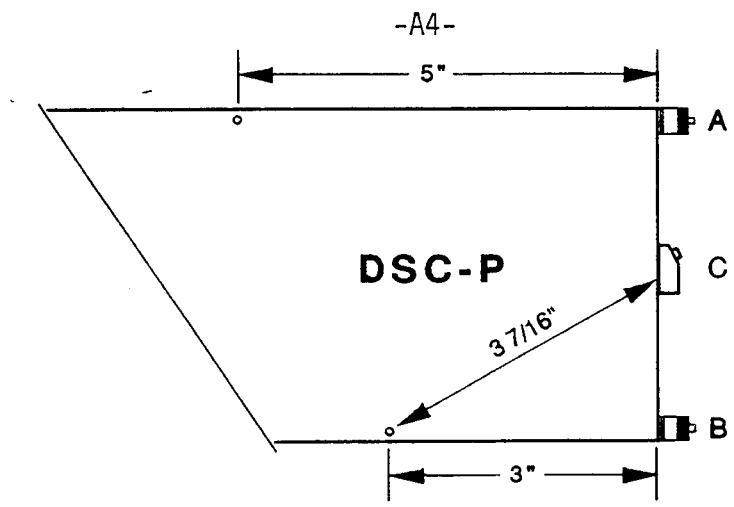


Figure A1.

- D = Pin Dia. in Inches
- E = Dia. of Root of Threads in Inches
- S = Depth of Shoulder to Root of Threads
- L = End of Pin to Far Shoulder
- T = Total Length of Pin
- M = Length of Threads

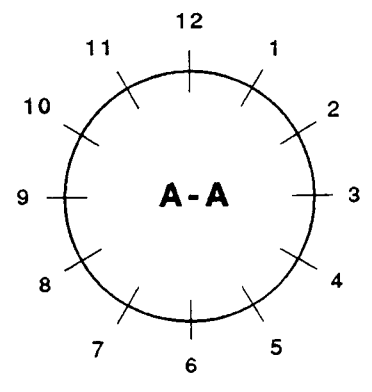
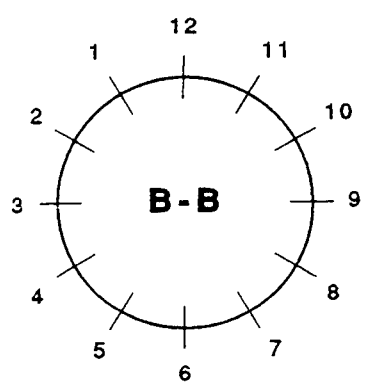
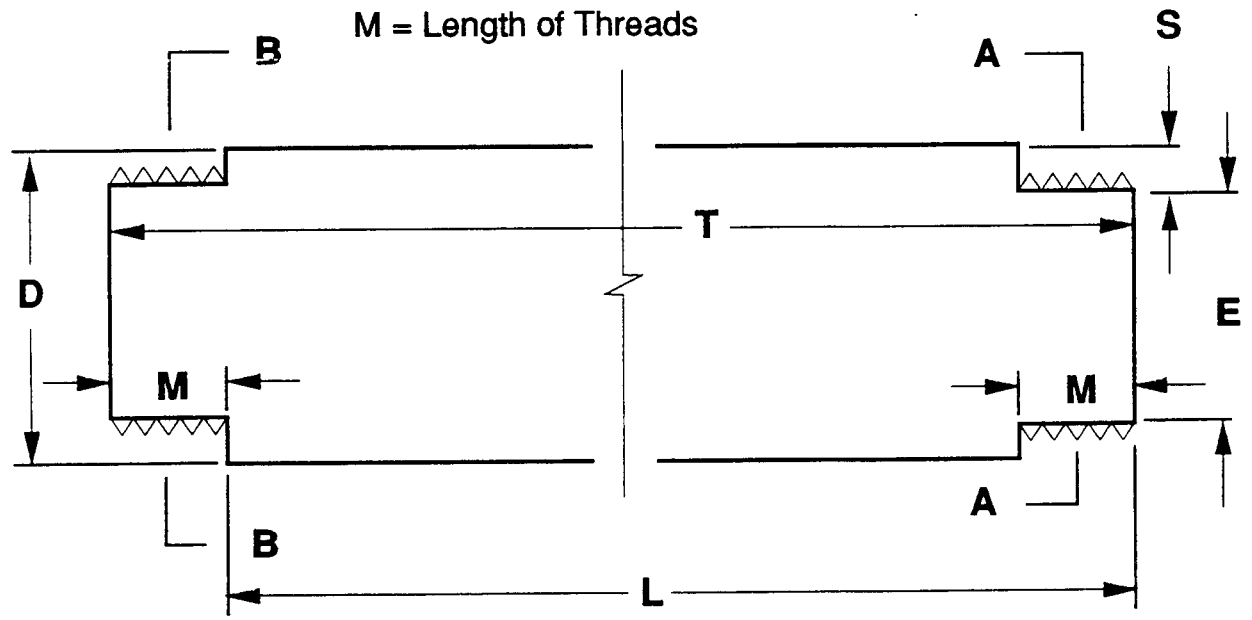


Figure A2.

APPENDIX B

G1 and G2 Condition Ratings

<u>Code</u>	<u>Condition</u>	<u>Angle Beam Indication Rating</u>	<u>Adjusted Straight Beam Indication Rating</u>	<u>Frequency Years</u>
8	VERY GOOD-No problems noted.	NI	NI	5
7	GOOD-Very minor surface rust, insignificant indications and high indication ratings.	above 8	NI	5
6	SATISFACTORY-Pitting, shallow corrosion or wear grooves but not affecting structural capacity.	4-8	NI	2
5	FAIR-Corrosion or wear grooves producing prob- able section loss which may affect structural capacity for over-loads.	4-8	6-15	2
4	POOR-Significant corrosion or wear grooves causing definite section loss.	0-3	6-15	*
3	SERIOUS-Deep corrosion or wear grooves causing significant section loss. Grooves below shoulders. Requires posting and investigation by structural engineer.	0-3	0-5	*
2	CRITICAL-Extreme section loss due to corrosion, wear grooves, or cracks present. Shore beams. Pins should be replaced. Lanes may be closed pending an investigation by a structural engineer.	-10 to -1	-4 to -1	*

<u>Code</u>	<u>Condition</u>	<u>Angle Beam Indication Rating</u>	<u>Adjusted Straight Beam Indication Rating</u>	<u>Frequency Years</u>
1	IMMINENT FAILURE-Pins partially severed. Structure or lane must be closed pending corrective action if more than 30% of beam lines so rated. Shore affected lines.	-20 to -1	-10 to -5	*
0	FAILED-Out of service. Deep fracture. Close structure/lane if more than 25% of lines so rated. Shore affected lines.	Below -20	Below -20	*

NI = No Indication

* Inspection interval and remedial action to be established by the Central Office considering the specific site characteristics.

The above are guides for coding the condition of pin and hanger assemblies in multi-girder steel bridges. The inspector must take into consideration the severity of the deficiency, the number of beams affected, and the number of adjacent beams with similiar deficiencies.